treatment or without Ca + AngII treatment and analyzed for smooth muscle α-actin (αSMA), nuclear NFκB, phospho-Stat3, phospho-Smad2 and CD45 (Fig. 5, Supplementary Figs. 9 and 10). Double labeling for αSMA and CD45 revealed that the majority of the αSMA-negative cells were CD45-positive inflammatory cells (Supplementary Fig. 9). Ca + AngII treatment caused slight increases in nuclear NFκB (from 6.6% to 7.2%) and phosho-Stat3 (from 1.8% to 3.5%), the major transcription factors for proinflammatory signaling, in αSMA-negative cells of WT aorta (Fig. 5a). Ca + AngII caused more prominent increases in nuclear NFκB (from 6.7% to 12.4%) and phosho-Stat3 (from 6.1% to 12.4%) in αSMA-negative cells of TNC-KO aorta, consistent with the exaggerated proinflammatory response. In contrast, nuclear phospho-Smad2, the downstream of TGFβ signal, was weaker in TNC-KO aorta both in αSMA-positive and -negative populations regardless of Ca + AngII treatment (Fig. 5A, Supplementary Fig. 10). Interestingly, although the ratio of αSMA-positive cells in total cell populations was comparable between WT and TNC-KO aortae without Ca + AngII treatment, TNC-KO aorta showed weaker expression αSMA (Fig. 5b). TNC-KO aorta showed more increase in the proportion of αSMA-negative cells, presumably CD45-positive inflammatory cells, than WT aorta by Ca + AngII treatment (Supplementary Fig. 9). This could be due to actual increase in αSMA-negative cells, decrease in αSMA-positive cells, or both. Further studies would be required to evaluate the effect of TNC on infiltration, survival and proliferation of various cell types. Taken together, reduced TGFβ signaling may underlie the abnormal response of TNC-KO aorta, including compromised tissue reinforcing response[18], reduced αSMA expression[19] and exaggerated proinflammatory response in aorta.

Discussion

In this study, we provided a new model of aortic stiffening, a known risk factor for AAD[8–10,20], that augments the hemodynamic stress elicited by AngII. Using this model, we demonstrated that TNC protects the aorta from AAD, but not from AAA, via two mechanisms. First, TNC supports the stress-induced expression of ECM that reinforce the aorta[21]. Second, TNC expression dampens the stress-induced excessive inflammatory response in the aorta (Fig. 6).

Although induction of TNC is associated with deposition of ECM during the inflammatory responses in cardiovascular[5,22] and other tissues with high mechanical stress[23], its significance in stress adaptation has been unclear. Our data indicate that TNC acts as a stress-evoked molecular damper that keeps the destructive stress response in check before AAD development (Fig. 4e). Exaggerated inflammatory response with higher IL-6 expression in the absence of TNC has also been reported in the brain injury model[24]. In addition, IL-6 has been reported to play a crucial role in AAD development[3].

It is noteworthy that *Tnc* deletion augmented NFκB and Stat3 activities mainly in αSMA-negative cells, most of which were CD45-positive inflammatory cells (Supplementary Figs. 9 and 10). On the other hand, *Tnc* deletion diminished Smad2 activity in both αSMA-positive and -negative cells. This cell type-specific effect of *Tnc* deletion could be due to a number of factors, including the changes in the cytokine environment and the sensitivity of a cell type to cytokines, which could be modulated by TNC. The diminished Smad2 activity indicates the impaired TGFβ signaling that regulates ECM biosynthesis[18] and smooth muscle differentiation[19] in TNC-KO aorta. Consistently, TNC-KO aorta showed reduction in basal αSMA expression and impairment of ECM gene inductions in response to the aortic stress, suggesting that TNC is involved in the normal function of aortic smooth muscle cells as proposed in the developing coronary arteries[25]. Thus, reduction in TGFβ signaling may be the underlying mechanism for AAD development in TNC-KO. Interestingly, genetic defect in tenascin-X, a constitutively expressed member of tenascin family, causes a recessive form of Ehlers-Danlos syndrome because of insufficient deposition of ECM and reduction in the tensile strength of the affected tissue[26]. TNC may function in the analogous way with tenascin-X in the tissue under high mechanical stress by facilitating the deposition of ECM to reinforce the tissue.

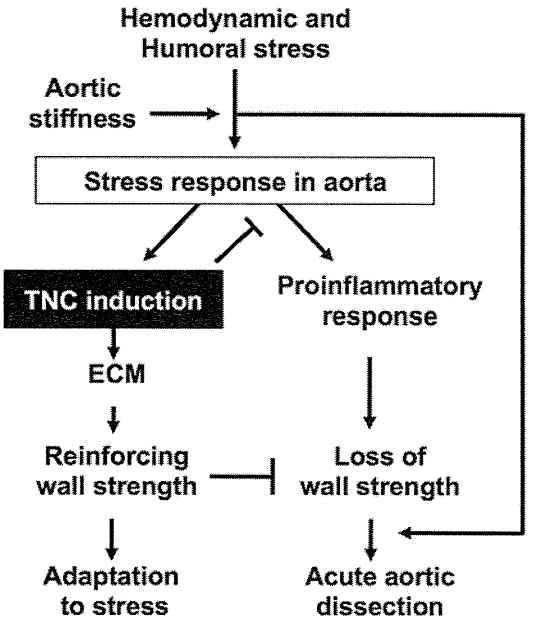

Figure 6 | Schematic diagram of TNC-mediated protection of the aorta. Aortic stress induces TNC expression, which in turn protects the aorta by reinforcing the wall strength of the aortic tissue and by suppressing an excessive proinflammatory response.

The limitation in this study is the different manifestation of AAD in mouse and human. The mouse AAD in this study showed the disruption of normally-looking intimomedial layer that recapitulates the pathological hallmark of human AAD. However, the mouse AAD did not recapitulate the longitudinal dissection of medial layers that follows the intimomedial layer disruption in human. This is most likely because the aortic wall in human consists of tens of elastic lamellar units whereas that of mice consists of only 3 to 4 units. Thus, disruption of a few elastic lamellar units results in the complete rupture of aorta rather than the tearing of medial layer. The progression of AAD subsequent to the intimomedial disruption would require future investigation, possibly in larger animals. Another difference is that most of human AAD develops in thoracic aorta, whereas most of the mouse AAD developed in suprarenal aorta in this and other studies[3,27]. A number of potential reasons for this could be considered, including the different hemodynamics in human and mouse, which require further studies. In this regard, it is noteworthy that intrinsic TNC expression is low in part of the ascending and descending aorta, the regions frequently affected in human AAD[1], even under the aortic stress with Ca + AngII treatment. The sharp boundary of the TNC expression pattern suggests the genetically programmed regulation. Whether human aorta have similar expression pattern of TNC, and how TNC expression is regulated in aorta also require future investigation.

Our data demonstrated that aortic stiffening augmented AngII-induced hemodynamic stress and stress response, concomitant with the increase in AAD incidence of TNC-KO mice. However, several questions remain to be answered regarding the mechanistic links among the aortic stiffening, hemodynamic stress and AAD development. First, the difference in AAD incidence caused by the aortic stiffening was relatively small, and the reproducibility of this finding should be tested possibly in other models of aortic stiffening. Second, although we used dP/dt as a readout of hemodynamic stress on aortic walls, further studies are required to investigate how aortic stiffening

influences other hemodynamic parameters. Third, it should be explored what types of hemodynamic stress are sensed by which types of cells in aortic walls, and how the stress is transduced to the responses of destructive inflammation and tissue reinforcement. Furthermore, aortic tissue is likely to have multiple mechanisms, in addition to TNC, to maintain the tissue integrity under various stress. Deciphering such protective mechanisms of the stressed aorta will provide insights into the pathogenesis of AAD, which is essential for developing better diagnostic and therapeutic strategies for this lethal disease.

Methods

Animal experiments. We maintained the TNC-KO mice by mating the heterozygous ($TNC^{+/-}$) pairs and performed experiments using the litter mates of $TNC^{+/+}$ (WT) and $TNC^{-/-}$ (TNC-KO) mice with comparable ages; 10–14 weeks of age at the beginning of Ca + AngII treatment. We used periaortic application of 0.5 M $CaCl_2$ to the infrarenal aorta to create a mouse model for stiffened aorta and infused the mice with AngII (1 μg/min/kg) for up to 4 weeks using osmotic minipump (Alzet model 1004) to apply pathological stress to the aorta[7]. Mice were killed by pentobarbital overdose at the indicated time points and blood and tissue samples were collected. The aortic tissue was excised either immediately for protein and mRNA expression analysis or after perfusion and fixation with 4% paraformaldehyde in PBS at physiological pressure for histological analysis. Enlargement of the aorta was defined when the diameter was equal to or exceeded the 1.5× of control aorta (control diameters; WT 0.75 ± 0.08 mm, KO 0.75 ± 0.02 mm). For the pressure-diameter analysis, aortae were excised and cleaned of peri-adventitial tissue without perfusion fixation. We used the Vevo 770 system (VisualSonics) to measure aortic wall motion in fluothane-anesthetized mice. We performed aortic catheterization of the fluothane-anesthetized mice for direct hemodynamic measurements using Mikro-Tip pressure catheters (Millar) and the PowerLab data acquisition system (Data Science Instruments), after adjusting the systolic blood pressure to approximately 100 mmHg at the most distal measurement point (5 mm above the iliac bifurcation).

Ethics statement. All animal experiment was performed in accordance with the guidelines approved by the ethics committees in Yamaguchi University, Kurume University and Mie University.

Cell culture experiments. We obtained suprarenal aortic smooth muscle cells (SMC) for culture from TNC-KO mice to avoid the influence of endogenous TNC. We isolated the SMCs by enzymatic dispersion, plated on the laminin-coated culture plates (20 μg/mL, 2 hrs at room temperature), and maintained them in Dulbecco's modified Eagle medium (DMEM) supplemented with 10% fetal bovine serum. We cultured TNC-KO aortic SMC in the presence or absence of exogenous TNC (10 μg/mL) and stimulated the cells with 10 ng/mL TNFα for 24 h before obtaining total RNA.

Expression analysis and dataset. Serum TNC levels were determined with an ELISA kit (Immuno-Biological Laboratories). Serum cytokine levels were determined with the Bio-Plex system (Bio-Rad). We isolated total RNA using RNeasy (Qiagen) from SMC culture or suprarenal aorta (from the edge of the right renal artery to approximately 7 mm above) cleaned of peri-adventitial loose connective tissue with intact medial and adventitial layers. We performed transcriptome analyses using the GeneChip Mouse Genome 430 2.0 (Affymetrix) and Microarray Analysis Suite (MAS) 5.0. We also performed quantitative reverse transcription-polymerase chain reaction (RT-PCR) using RT^2 Profiler PCR Array System (Qiagen).

Morphological and functional analyses. We obtained high-resolution optical section images of the excised aorta using an optical coherence tomography (OCT) imaging system (Goodman). We used OsiriX Imaging Software (OsiriX) for three-dimensional reconstruction of the optical sections. For pressure-diameter analysis of the aorta, we ligated the branches of the excised aorta and placed it in a PBS bath on the microscope connected to a charge-coupled device camera. We applied 0–200 mmHg of intra-aortic pressure with a syringe and monitored the external diameters of the aorta with the PowerLab data acquisition system. We observed paraffin-embedded sections of aortic tissue with elastica van Gieson (EVG). For the quantitative analysis of collagen deposition, we stained the aortic tissue sections by picrosirius red. Aortic media, as determined by the area between the innermost and outermost elastic lamellae, was manually traced on the computer images. The collagen deposition area, as determined by the picrosirius red staining, and medial area were measured using ImagePro software (Media Cybernetics). We determined the pattern of *Tnc* gene activity by Bluo-Gal staining of aortae from heterozygous *Tnc* reporter mice in which the *LacZ* gene encoding β-galactosidase was knocked-in to one of the *Tnc* loci[13].

Imaging cytometry and immunohistochemistry. We performed imaging cytometric analysis using ArrayScan XTI (Thermo Fisher Scientific) for mouse aortae 1 week after the Ca + AngII treatment. Two aortic tissue sections were obtained from each mouse; WT (control; n = 4, Ca + AngII; n = 3) and TNC-KO (control; n = 5, Ca + AngII; n = 5). The tissue sections were stained for either NFκB (Cell Signaling Technologies), phospho-Stat3 (P-Tyr705, Cell Signaling Technologies), phospho-Smad2 (P-Ser465/467, Millipore) and CD45 (Abcam) antibodies with TSA labeling kit with AlexaFluor 488 tyramide (Invitrogen). All of the tissue sections were stained for smooth muscle α-actin (αSMA; Sigma-Aldrich) with DyLight 549-labeled secondary antibody (Jackson ImmunoResearch) and nuclei with DAPI. On average 339 cells/mouse were counted to obtain the cytometric data. For αSMA staining, the same staining and image acquisition protocols were used for all of the samples. For NFκB, phospho-Stat3, phospho-Smad2 and CD45, the staining protocols were optimized for individual target molecules, and a constant image acquisition protocol was used within the same target molecule. The cytometric data obtained by ArrayScan XTI were analyzed by FlowJo software. Immunohistochemical stainings were performed for type 1 collagen (LSL), fibronectin (Sigma-Aldrich) and lysyl oxidase (US Biological).

Statistical analysis. All data are expressed as means ± SD. Statistical analysis was performed with Mann-Whitney test for the comparisons of 2 groups, Kruskal-Wallis test for multiple groups and Friedman test for the pressure-dimension analysis. Post test was performed by Dunn's multiple comparison test. The chi-square test was used where appropriate. $P < 0.05$ was considered to be significant.

1. Cronenwett, J. L. & Johnston, W. *Rutherford's Vascular Surgery.* 7th edn, (Saunders, 2010).
2. Dietz, H. C. TGF-beta in the pathogenesis and prevention of disease: a matter of aneurysmic proportions. *J Clin Invest* **120**, 403–407 (2010).
3. Tieu, B. C. *et al.* An adventitial IL-6/MCP1 amplification loop accelerates macrophage-mediated vascular inflammation leading to aortic dissection in mice. *J Clin Invest* **119**, 3637–3651 (2009).
4. Bush, E. *et al.* CC chemokine receptor 2 is required for macrophage infiltration and vascular hypertrophy in angiotensin II-induced hypertension. *Hypertension* **36**, 360–363 (2000).
5. Kimura, T. *et al.* Tenascin-C is expressed in abdominal aortic aneurysm tissue with an active degradation process. *Pathol Int* **61**, 559–564 (2011).
6. Longo, G. M. *et al.* Matrix metalloproteinases 2 and 9 work in concert to produce aortic aneurysms. *J Clin Invest* **110**, 625–632 (2002).
7. Yoshimura, K. *et al.* Regression of abdominal aortic aneurysm by inhibition of c-Jun N-terminal kinase. *Nat Med* **11**, 1330–1338 (2005).
8. Khau Van Kien, P. *et al.* Mapping of familial thoracic aortic aneurysm/dissection with patent ductus arteriosus to 16p12.2-p13.13. *Circulation* **112**, 200–206 (2005).
9. Nollen, G. J., Groenink, M., Tijssen, J. G., Van Der Wall, E. E. & Mulder, B. J. Aortic stiffness and diameter predict progressive aortic dilatation in patients with Marfan syndrome. *Eur Heart J* **25**, 1146–1152 (2004).
10. Cavalcante, J. L., Lima, J. A., Redheuil, A. & Al-Mallah, M. H. Aortic stiffness: current understanding and future directions. *J Am Coll Cardiol* **57**, 1511–1522 (2011).
11. Mackie, E. J. *et al.* Expression of tenascin by vascular smooth muscle cells. Alterations in hypertensive rats and stimulation by angiotensin II. *Am J Pathol* **141**, 377–388 (1992).
12. Chiquet-Ehrismann, R. & Chiquet, M. Tenascins: regulation and putative functions during pathological stress. *J Pathol* **200**, 488–499 (2003).
13. Saga, Y., Yagi, T., Ikawa, Y., Sakakura, T. & Aizawa, S. Mice develop normally without tenascin. *Genes Dev* **6**, 1821–1831 (1992).
14. Huang da, W., Sherman, B. T. & Lempicki, R. A. Systematic and integrative analysis of large gene lists using DAVID bioinformatics resources. *Nat Protoc* **4**, 44–57 (2009).
15. de Vega, S., Iwamoto, T. & Yamada, Y. Fibulins: multiple roles in matrix structures and tissue functions. *Cell Mol Life Sci* **66**, 1890–1902 (2009).
16. Verrecchia, F., Wagner, E. F. & Mauviel, A. Distinct involvement of the Jun-N-terminal kinase and NF-kappaB pathways in the repression of the human COL1A2 gene by TNF-alpha. *EMBO Rep* **3**, 1069–1074 (2002).
17. Yokoyama, U. *et al.* Prostaglandin E2 Inhibits Elastogenesis in the Ductus Arteriosus via EP4 Signaling. *Circulation* **129**, 487–496 (2014).
18. Bobik, A. Transforming growth factor-betas and vascular disorders. *Arteriosclerosis, thrombosis, and vascular biology* **26**, 1712–1720 (2006).
19. Kumar, M. S. & Owens, G. K. Combinatorial control of smooth muscle-specific gene expression. *Arteriosclerosis, thrombosis, and vascular biology* **23**, 737–747 (2003).
20. Hiratzka, L. F. *et al.* 2010 ACCF/AHA/AATS/ACR/ASA/SCA/SCAI/SIR/STS/SVM guidelines for the diagnosis and management of patients with Thoracic Aortic Disease: a report of the American College of Cardiology Foundation/American Heart Association Task Force on Practice Guidelines, American Association for Thoracic Surgery, American College of Radiology, American Stroke Association, Society of Cardiovascular Anesthesiologists, Society for Cardiovascular Angiography and Interventions, Society of Interventional Radiology, Society of Thoracic Surgeons, and Society for Vascular Medicine. *Circulation* **121**, e266–369 (2010).
21. Curci, J. A., Baxter, B. T. & Thompson, R. W. in *Vascular Surgery* (ed Rutherford, R. B.) 475–492 (Saunders, 2005).
22. Imanaka-Yoshida, K. Tenascin-C in cardiovascular tissue remodeling: from development to inflammation and repair. *Circ J* **76**, 2513–2520 (2012).

23. Carey, W. A., Taylor, G. D., Dean, W. B. & Bristow, J. D. Tenascin-C deficiency attenuates TGF-beta-mediated fibrosis following murine lung injury. *Am J Physiol Lung Cell Mol Physiol* **299**, L785–793 (2010).
24. Ikeshima-Kataoka, H., Shen, J. S., Eto, Y., Saito, S. & Yuasa, S. Alteration of inflammatory cytokine production in the injured central nervous system of tenascin-deficient mice. *In Vivo* **22**, 409–413 (2008).
25. Ando, K. *et al.* Tenascin C may regulate the recruitment of smooth muscle cells during coronary artery development. *Differentiation* **81**, 299–306 (2011).
26. Burch, G. H. *et al.* Tenascin-X deficiency is associated with Ehlers-Danlos syndrome. *Nature genetics* **17**, 104–108 (1997).
27. Shen, Y. H. *et al.* AKT2 confers protection against aortic aneurysms and dissections. *Circulation research* **112**, 618–632 (2013).

Acknowledgments

We thank Ms. Oishi, Ms. Hozawa and Ms. Nishino (Yamaguchi University), Ms. Kogure, Ms. Nishigata and Ms. Kimura (Kurume University), Ms. Hara, and Ms. Namikata (Mie University) for their technical expertise and Ms. Kiyohiro (Kurume University) for administrative assistance. Funding: This work was supported in part by KAKENHI and by a Grant-in-Aid for the Strategic Research Foundation in Private Universities from MEXT Japan, a Grant for Intractable Disease from Ministry of Health, Labour and Welfare of Japan, a grant from the Vehicle Racing Commemorative Foundation, a grant from the Uehara Memorial Foundation and a grant from the Daiichi Sankyo Company.

Author contributions

T.K., K.Y., A.F., S.I., S.H. and N.N. performed the animal experiments. K.S. and Y.I. performed the aortic catheterization. K.I.-Y. and T.Y. maintained the TNC-KO mice and performed the histopathological analyses. T.U. performed the optical coherence tomography. T.M. performed the bioinformatic analysis. K.H., M.H., K.A., M.M. and T.I. provided scientific advice. H.A., K.Y., K.I.-Y. and M.H. designed this study. H.A. wrote the manuscript.

Additional information

Supplementary information accompanies this paper at http://www.nature.com/scientificreports

Competing financial interests: The authors declare no competing financial interests.

How to cite this article: Kimura, T. *et al.* Tenascin C protects aorta from acute dissection in mice. *Sci. Rep.* **4**, 4051; DOI:10.1038/srep04051 (2014).

PLOS ONE

Periostin Links Mechanical Strain to Inflammation in Abdominal Aortic Aneurysm

Osamu Yamashita[1], Koichi Yoshimura[1,2]*, Ayako Nagasawa[1], Koshiro Ueda[1], Noriyasu Morikage[1], Yasuhiro Ikeda[3], Kimikazu Hamano[1]

1 Department of Surgery and Clinical Science, Yamaguchi University Graduate School of Medicine, Ube, Japan, **2** Graduate School of Health and Welfare, Yamaguchi Prefectural University, Yamaguchi, Japan, **3** Department of Medicine and Clinical Science, Yamaguchi University Graduate School of Medicine, Ube, Japan

Abstract

Aims: Abdominal aortic aneurysms (AAAs) are characterized by chronic inflammation, which contributes to the pathological remodeling of the extracellular matrix. Although mechanical stress has been suggested to promote inflammation in AAA, the molecular mechanism remains uncertain. Periostin is a matricellular protein known to respond to mechanical strain. The aim of this study was to elucidate the role of periostin in mechanotransduction in the pathogenesis of AAA.

Methods and Results: We found significant increases in periostin protein levels in the walls of human AAA specimens. Tissue localization of periostin was associated with inflammatory cell infiltration and destruction of elastic fibers. We examined whether mechanical strain could stimulate periostin expression in cultured rat vascular smooth muscle cells. Cells subjected to 20% uniaxial cyclic strains showed significant increases in periostin protein expression, focal adhesion kinase (FAK) activation, and secretions of monocyte chemoattractant protein-1 (MCP-1) and the active form of matrix metalloproteinase (MMP)-2. These changes were largely abolished by a periostin-neutralizing antibody and by the FAK inhibitor, PF573228. Interestingly, inhibition of either periostin or FAK caused suppression of the other, indicating a positive feedback loop. In human AAA tissues in *ex vivo* culture, MCP-1 secretion was dramatically suppressed by PF573228. Moreover, *in vivo*, periaortic application of recombinant periostin in mice led to FAK activation and MCP-1 upregulation in the aortic walls, which resulted in marked cellular infiltration.

Conclusion: Our findings indicated that periostin plays an important role in mechanotransduction that maintains inflammation via FAK activation in AAA.

Citation: Yamashita O, Yoshimura K, Nagasawa A, Ueda K, Morikage N, et al. (2013) Periostin Links Mechanical Strain to Inflammation in Abdominal Aortic Aneurysm. PLoS ONE 8(11): e79753. doi:10.1371/journal.pone.0079753

Editor: Elena Aikawa, Brigham and Women's Hospital, Harvard Medical School, United States of America

Received July 30, 2013; **Accepted** September 30, 2013; **Published** November 19, 2013

Funding: This work was supported by a Grant-in-Aid for Scientific Research from the Japan Society for the Promotion of Science (KAKENHI 24390302 and 22659232 to KY), the Takeda Science Foundation (to KY), and the Uehara Memorial Foundation (to KY). The funders had no role in study design, data collection and analysis, decision to publish, or preparation of the manuscript.

Competing Interests: The authors have declared that no competing interests exist.

* E-mail: yoshimko@yamaguchi-u.ac.jp

Introduction

Abdominal aortic aneurysm (AAA) is a common disease that causes segmental expansion and rupture of the aorta with a high mortality rate [1,2]. Currently, therapeutic options for AAA are limited to open or endovascular surgical repair to prevent the catastrophic event of rupture [3]. The lack of nonsurgical treatment represents an unmet need, particularly in terms of pharmacotherapy [2,4]. The development of biomarkers for AAA is also essential to produce clinically practical pharmacotherapy [2,5]. It is generally accepted that an AAA is characterized by chronic inflammation and extracellular matrix degradation caused by proteolytic enzymes, such as matrix metalloproteinases (MMPs) [6,7]. In addition, it was reported that successful endovascular aneurysm repair caused decreases in the size of the AAA and in plasma MMPs levels [8]. This suggested that mechanical stress is critical for maintaining disease activity in AAA, and that the signaling pathway stimulated by mechanical stress represents a therapeutic target. However, the molecular mechanisms that regulate mechanotransduction in AAA remain largely unknown.

Periostin is a matricellular protein, which belongs to the fasciclin I family. Periostin interacts with integrin molecules, including $\alpha v\beta 3$ and $\alpha v\beta 5$, on cell surfaces, which provides signals for tissue development and remodeling [9]. Previously, it was shown that periostin was upregulated by mechanical strain in cultured cells [10,11] and also that periostin promoted the secretion of MMPs from cardiac cells [12]. These findings led to the hypothesis that periostin may play a role in the mechanotransduction involved in the pathogenesis of AAA. In the present study, we demonstrated for the first time that periostin mediated the inflammatory responses to mechanical strain in AAA in human tissue specimens, cultured vascular smooth muscle cells (VSMCs), and an *in vivo* mouse model.

Methods

Human aortic samples

We obtained abdominal aortic wall specimens from 42 patients with AAA that underwent open surgical repair. As controls, non-aneurysmal abdominal aortic wall specimens were obtained from 5

patients that underwent aortic surgery. The groups with and without AAA were not significantly different in age (74±1 vs. 68±5 years, $p=0.27$), the proportion of males (76 vs. 60%, $p=0.43$), or the prevalence of cigarette smoking (71 vs. 60%, $p=0.60$). Also, patients with and without AAA were not significantly different in the prevalence of hypertension (73 vs. 60%, $p=0.56$), diabetes mellitus (23 vs. 20%, $p=0.90$), or dyslipidemia (23 vs. 20%, $p=0.72$). The aortic tissue specimens were used for protein analyses by western blotting, immunohistochemistry, and *ex vivo* organ cultures, as previously described [13,14]. All patients provided written informed consent, in accordance with the principles outlined in the Declaration of Helsinki. All experimental protocols with human specimens were approved by the Institutional Review Board at Yamaguchi University Hospital (#H24-26).

Western blotting

Protein extraction and western blotting were performed as described previously [13,14]. Briefly, equal amounts of sample proteins were loaded onto individual lanes in sodium dodecyl sulfate polyacrylamide gels, separated by electrophoresis, and transferred onto polyvinylidene difluoride membranes. Membranes were probed with antibodies against periostin (BioVendor, Brno, Czech Republic), monocyte chemoattractant protein-1 (MCP-1) (Cell Signaling Technology, Danvers, MA, USA), focal adhesion kinase (FAK) (Cell Signaling Technology), phosphorylated FAK (Tyr397) (Abcam, Cambridge, UK), extracellular signal-regulated kinase (ERK) (R&D Systems, Minneapolis, MN, USA), phosphorylated ERK (Promega, Madison, WI, USA), c-Jun N-terminal kinase (JNK) (Santa Cruz Biotechnology, Dallas, TX, USA), phosphorylated JNK (Promega), and glyceraldehyde 3-phosphate dehydrogenase (GAPDH) (Millipore, Billerica, MA, USA).

Histological and immunohistochemical analyses

Paraffin-embedded sections were stained with hematoxylin/eosin (HE), Masson trichrome (MT), and elastica-van Gieson (EVG) stains for histological analysis. Sections were also probed with antibodies raised against appropriate antigens for immunohistochemistry, as described previously [13,14]. We detected periostin, α-smooth muscle actin (α-SMA), MCP-1, and phosphorylated FAK (pFAK) by probing sections with anti-periostin antibody (BioVendor), anti-smooth muscle α-actin antibody (Sigma-Aldrich, St. Louis, MO, USA), anti-MCP-1 antibody (R&D Systems), and anti-pFAK antibody (Abcam), respectively.

Gelatin zymography

Gelatin zymography was performed as described previously [13,14]. The protein levels of MMP-2 and MMP-9 were determined by quantifying clear bands of the corresponding size.

Enzyme-linked immunosorbent assay (ELISA)

The concentrations of MCP-1 in conditioned media were quantified by a sandwich enzyme immunoassay technique using the rat MCP-1 ELISA Kit (Thermo Scientific, Rockford, IL, USA) and the human MCP-1 ELISA Kit (R&D Systems), according to the manufacturer's instructions.

VSMC culture and mechanical strain experiments

Rat aortic VSMCs derived from the media of healthy rat aorta were purchased from Cell Applications, Inc (San Diego, CA, USA). VSMCs were maintained in Dulbecco's modified Eagle's medium (DMEM) with 10% fetal bovine serum. Before experiments, VSMCs were seeded in a laminin-coated silicon chamber and serum-starved for 24 h. Then, we applied cyclic, uniaxial strain to the VSMCs with a stretching system (STB-140-10) (STREX, Osaka, Japan). We divided the VSMCs into three groups of cells to test different amounts of strain. Each group received 2%, 5%, or 20% stretching along the long axis (elongation) at a frequency of 30 cycles/min for 48 h. For inhibition studies, 1 μg/ml of periostin-neutralizing antibody (R&D Systems) or 10 μM of FAK inhibitor (PF573228) (Tocris Bioscience, Bristol, UK) was added to the medium 2 h before stretching. In one experiment, VSMCs were stimulated with 1 μg/ml of recombinant mouse periostin (R&D Systems) for 48 h.

Ex vivo cultures of human AAA specimens

The *ex vivo* organ culture was performed as described previously [13,14]. Briefly, the AAA wall specimens were minced into approximately 1-mm thick. Equal wet weights of the minced tissue were placed in each well of 12-well plates and cultured with serum-free DMEM. For the inhibition study, 10 μM of FAK inhibitor (PF573228) (Tocris Bioscience) was added to the medium for 48 h.

Animal experiments

For an observational study of changes in periostin levels during AAA development, we induced AAA in mice by periaortic application of 0.5 M $CaCl_2$, as described previously [13,15]. In the other study, we placed Gelfoam patches (3.5×2×2 mm) (Pfizer, New York, NY, USA) that contained 15 μg of recombinant mouse periostin (R&D Systems) in the periaortic space of mice for 7 days. Gelfoam patches with phosphate-buffered saline (PBS) served as the control. For both these studies, 7-week old, C57BL/6 male mice were anesthetized with an intraperitoneal injection of sodium pentobarbital (40 mg/kg) before undergoing a laparotomy. Anesthesia was monitored by periodic observation of respiration and the pain response. At the indicated time points, the experimental mice were sacrificed with an overdose of sodium pentobarbital (100 mg/kg, intraperitoneal injection). After a whole-body perfusion fixation with 4% paraformaldehyde in PBS at physiological pressure, the abdominal aortas were excised immediately for histological analysis. All experiments were performed in conformity with the Guide for the Care and Use of Laboratory Animals published by the United States National Institutes of Health, and the protocols were approved by the Yamaguchi University School of Medicine Animal Experiments Review Board (#31-068, #31-088).

Statistical analysis

All data are expressed as mean ± standard error (SE). Statistical analyses were performed with the Student's t-test, Mann-Whitney U test, or an analysis of variance (ANOVA), as appropriate. The post-test comparisons were performed with Bonferroni's method.

Results

Expression of periostin in human AAAs

First, we used western blotting to examine periostin protein levels in the walls of human AAA specimens. Compared to periostin levels in non-aneurysmal aortic walls (controls), periostin expression was significantly increased in the walls with AAA (**Fig. 1A**). However, we found no significant correlation between periostin expression and the diameter of AAA (data not shown); this lack of correlation was probably due to the heterogeneous pathology of AAA tissues. We also analyzed the localization of periostin within tissues to examine pathological changes that might be associated with increased periostin expression in AAA. All the

typical pathological processes of AAA were included in longitudinal strips of the walls of human AAA specimens that extended from a non-dilated area through a transitional area to a dilated area [2,15]. The non-dilated area showed preserved elastic lamellae with few inflammatory cells. The transitional area showed fragmented elastic fibers and severe cellular infiltration. The dilated area showed a marked loss of elastic lamellae and an increase in collagen fibers. Periostin expression was highest in the transitional area, where there was a gradual loss of elastic fibers and marked inflammatory cell infiltration (**Fig. 1B**). In addition, periostin and α-SMA, a marker for VSMCs, were mostly co-localized in human AAA wall specimens (**Fig. 1C**). Thus, our findings demonstrated that periostin was upregulated in human AAA wall specimens, particularly in the region of active inflammation.

Temporal pattern of periostin expression during AAA progression in a mouse model

Next, we analyzed a mouse model of AAA to evaluate periostin expression during the development and progression of AAA. The mouse model of AAA was created by periaortic application of $CaCl_2$ in the infrarenal aorta; this caused chronic inflammation of the aortic wall and resulted in fusiform dilation of the aorta (**Fig. 2A**). After 28 and 42 days, the maximum diameter of the infrarenal aorta was significantly increased compared to controls (**Fig. 2B**). In the initial 7 days, periostin expression in the aorta was increased both in controls and in the AAA model mice; then, at 14 days, periostin returned to nearly basal levels. These data indicated that periostin was transiently induced after the surgical procedures and/or $CaCl_2$ treatment. Interestingly, at 28 and 42 days, periostin expression once more increased, but only in the AAA model mice. At that same time, marked increases were noted in the aortic diameter, the inflammatory cell infiltration, and the destruction of elastic lamellae in AAA model mice (**Fig. 2C**). These results indicated that periostin was upregulated during the progression of AAA, particularly at the times that active inflammation was causing destruction of the extracellular matrix.

Role of periostin in linking mechanical strain to inflammatory responses in VSMCs

To examine the role of periostin in mechanotransduction, we used cultured VSMCs as an experimental system. We chose VSMCs, because periostin expression had co-localized mainly with α-SMA in human AAA specimens. We applied cyclic, uniaxial strain at 30 cycles/min to VSMCs cultured on silicone rubber membranes. We found that 20% cyclic strain strikingly upregulated periostin protein expression in VSMCs (**Fig. 3A**), but not 2% or 5% strain (data not shown). The 20% cyclic strain also resulted in a significant increase in MCP-1 protein expression (**Fig. 3B**) and increased secretion of the active form of MMP-2 (**Fig. 3C**). Intriguingly, these increases in both MCP-1 and active MMP-2 induced by cyclic strain were completely abrogated when cells were pre-treated with periostin-neutralizing antibody (**Fig. 3B-C**). These data demonstrated an essential role for periostin in linking mechanical strain to upregulation of MCP-1 and active MMP-2 in VSMCs. Moreover, when VSMCs were treated with recombinant periostin (rPeriostin), secretion of MCP-1 was potently induced (**Fig. 3J**). Collectively, these results indicated that upregulation of periostin in response to mechanical strain was both necessary and sufficient for MCP-1 secretion from VSMCs. This effect could potentially lead to inflammatory cell infiltration.

Role of periostin in mechanotransduction through FAK signaling in VSMCs

To understand the molecular mechanism that linked periostin to inflammatory responses, we focused on FAK; FAK has been reported to be activated by periostin [16,17] and to stimulate MCP-1-mediated inflammatory cell recruitment [18]. Therefore, we stimulated VSMCs with 20% cyclic uniaxial strain and examined FAK activation by western blotting with an anti-pFAK antibody. We found that cyclic strain induced significant FAK activation without changing the total FAK levels in VSMCs, and this was abrogated by pre-treatment with a periostin-neutralizing antibody (**Fig. 3D, G**). These results indicated that periostin was essential for FAK activation induced by mechanical strain. Similarly, cyclic strain induced significant activation of ERK and JNK, two major signaling molecules that can regulate inflammation-associated gene expression in VSMCs. This effect was also abrogated by pre-treating with periostin-neutralizing antibody (**Fig. 3E-F, H-I**).

We next used PF573228, a FAK inhibitor, to elucidate the molecular hierarchy in the network that links mechanical strain to inflammatory signaling through periostin. As reported previously, PF573228 entirely blocked activation of FAK by inhibiting its phosphorylation without changing total FAK levels (**Fig. 4A-B**). We found that PF573228 significantly prevented activation of ERK and JNK in response to mechanical strain applied to VSMCs (**Fig. 4A, C-D**). In addition, PF573228 blocked the mechanical strain-induced increases in both MCP-1 secretion and MMP-2 activity (**Fig. 4A, E-F**). Collectively, these findings indicated that the periostin/FAK axis was critical for activation of ERK and JNK and for increases in MCP-1 and active MMP-2 secretion in response to mechanical strain applied to VSMCs. Importantly, inhibition of FAK with PF573228 blocked the upregulation of periostin induced by mechanical strain (**Fig. 4A, G**), and inhibition of periostin with the neutralizing antibody blocked activation of FAK (**Fig. 3D**). Therefore, these findings revealed a vicious cycle between periostin and FAK that could amplify the inflammatory responses to mechanical strain in VSMCs.

Role of periostin/FAK axis in sustaining inflammatory responses in human AAA tissues

We confirmed that the periostin/FAK axis played a role in the inflammatory responses in the walls of human AAA specimens in *ex vivo* cultures. Because there may be considerable differences in the pathophysiology of disease in humans and animal models, *ex vivo* cultures of human AAA tissues offered the great advantage of being able to analyze the response to an applied agent directly in human tissues [13,19,20]. We found that, in *ex vivo* cultures, human AAA tissues maintained considerable levels of FAK, ERK, and JNK activities and MCP-1 and MMP secretions during the experiments (**Fig. 5A-F**). We applied PF573228 to inhibit the periostin/FAK axis in human AAA tissues and confirmed that PF573228 permeated AAA tissues and blocked phosphorylation of FAK successfully (**Fig. 5A**). Additionally, PF573228 caused significant reductions in the activation levels of ERK and JNK in human AAA tissues (**Fig. 5B-C**). Also, PF573228 reduced the secretion of MCP-1 and MMP-9 from human AAA tissues (**Fig. 5D-E**). However, PF573228 did not affect the secretion levels of total MMP-2 (**Fig. 5F**); this result suggested that the viability of human AAA tissues in *ex vivo* cultures was preserved after treatment with PF573228. These data clearly demonstrated an essential role for the periostin/FAK axis in sustaining inflammatory responses in human AAA tissues.

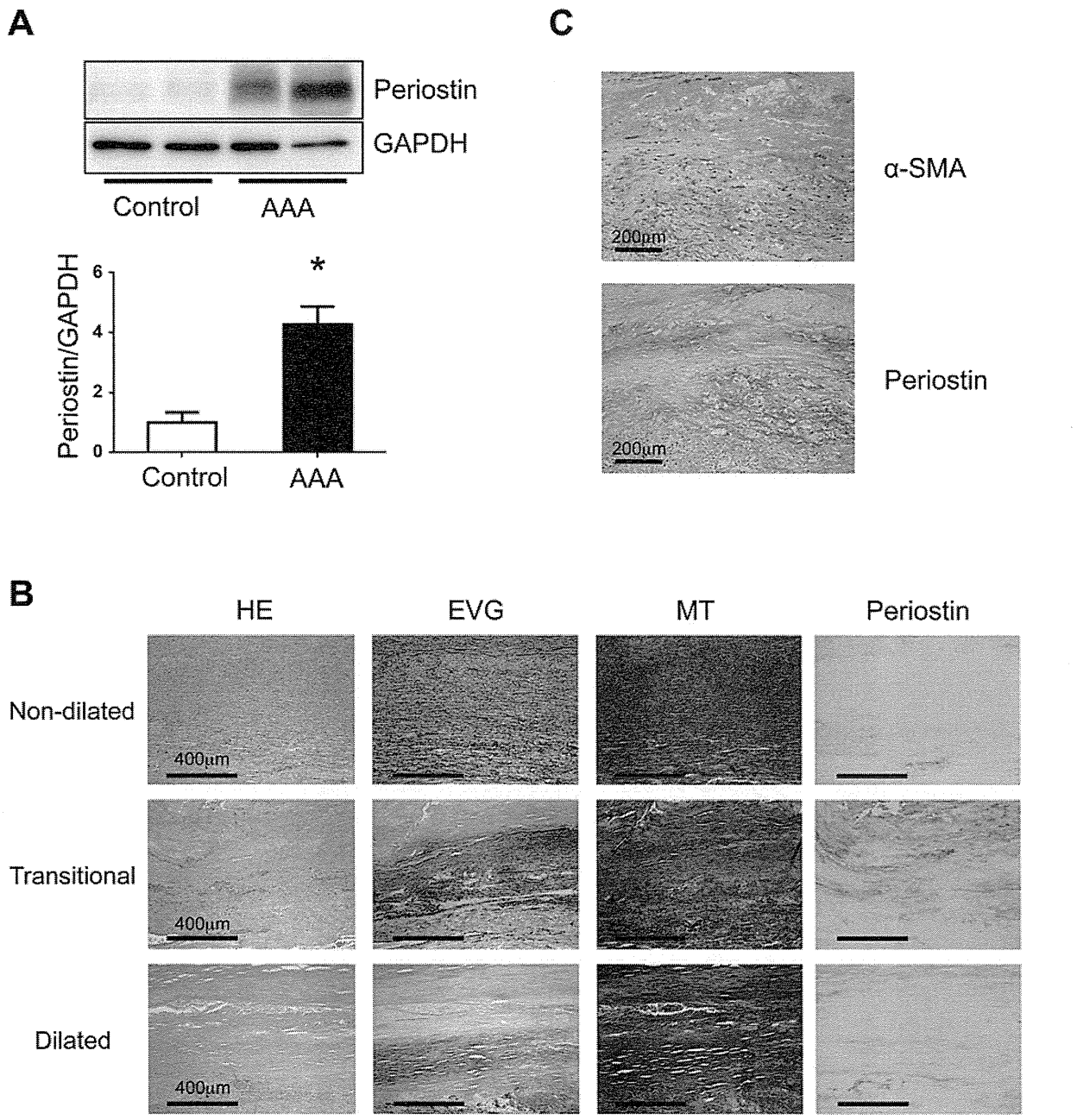

Figure 1. Expression of periostin in human AAA specimens. A: Protein samples were obtained from the walls of human AAA specimens (n = 42) and non-aneurysmal aortic walls (Control, n = 5). Representative western blot results for periostin are shown (top panel) with quantitative analyses (bottom panel). GAPDH served as an internal control. Data are mean ± SE. *$p<0.05$ compared to Control. **B**: Representative histological and immunohistochemical stains are shown for the walls of human AAA specimens. Different regions of the aorta include parts that are non-dilated (ND), transitional (T), and maximally dilated (MD). The luminal surface is oriented toward the top of each panel. Hematoxylin/eosin (HE), elastica van-Gieson (EVG), and Masson trichrome (MT) stains depict cell nuclei (blue-black), elastin network (black), and collagen fibers (blue), respectively. Localization of periostin is indicated by red staining. **C**: Localization of periostin and α-smooth muscle actin (α-SMA) is indicated by red staining.
doi:10.1371/journal.pone.0079753.g001

Role of periostin in inducing MCP-1-mediated inflammatory responses *in vivo*

Based on the findings from our studies *in vitro* and *ex vivo*, we investigated whether periostin could sufficiently induce inflammatory responses in mouse aortas *in vivo*. To that end, we associated rPeriostin with Gelfoam, a biodegradable extracellular matrix preparation. This provided a local delivery system for rPeriostin, as reported previously [21]. We implanted Gelfoam patches loaded with rPeriostin or with buffer (control) into the periaortic spaces of mice, and then examined inflammatory responses after 7 days. Immunohistochemical analysis revealed that the periostin protein levels were significantly higher in rPeriostin-treated aortas; the antibodies may have reacted with both endogenous and exogenous periostin. Compared to control aortas, rPeriostin-treated aortas showed dramatically higher levels of FAK activation and MCP-1 expression, both in cells of the aortic wall and in cells

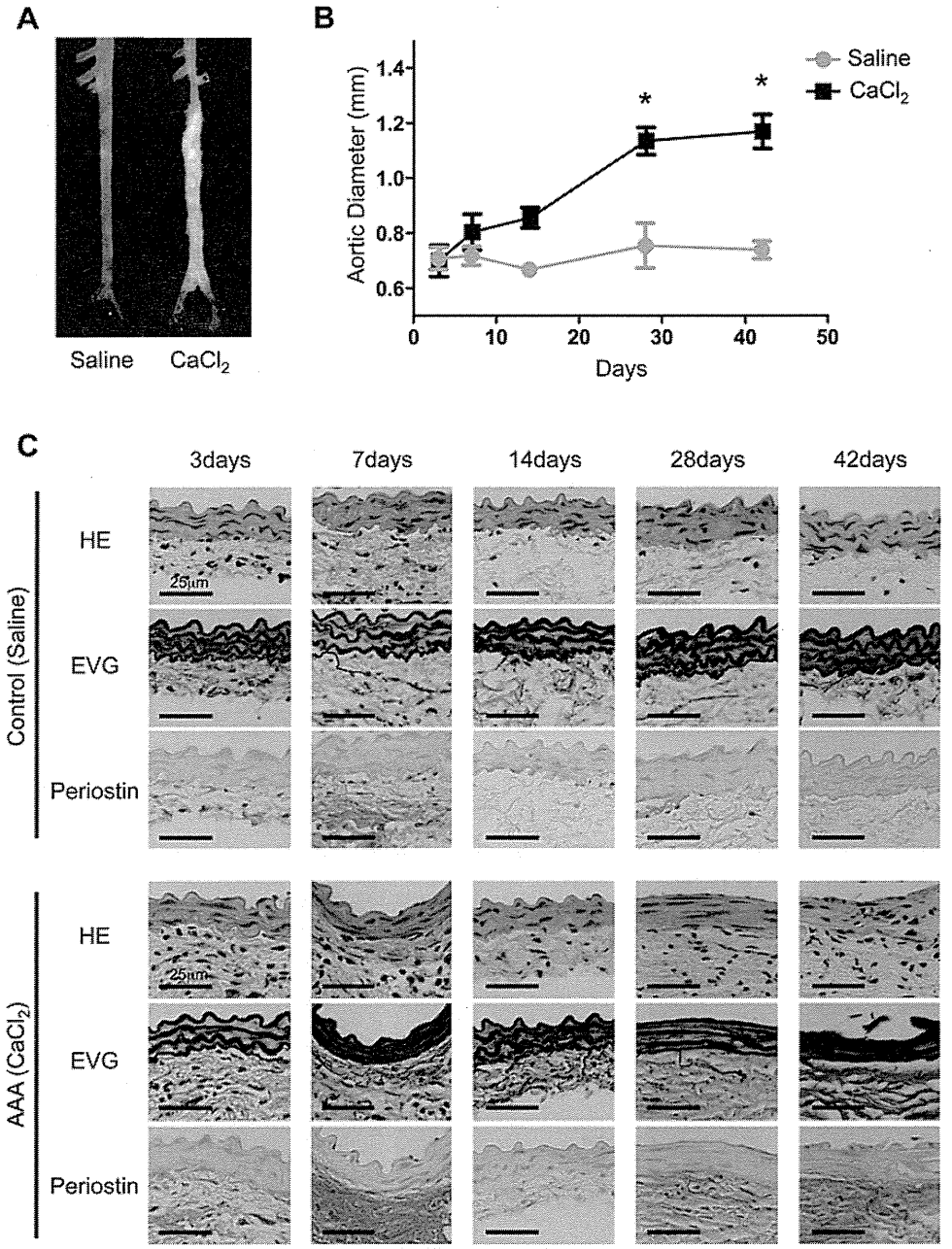

Figure 2. Temporal pattern of periostin expression during the development of abdominal aortic aneurysm (AAA) in a mouse model. A: Representative photographs show mouse abdominal aortas 42 days after periaortic application of saline (control) or $CaCl_2$ (for AAA induction). B: Changes in the diameters of abdominal aortas are shown for the indicated time points after application of saline or $CaCl_2$ (3 days, n = 3; 7 days, n = 4; 14 days, n = 4; 28 days, n = 3–4; 42 days, n = 7–8). Data are mean ± SE. *$p<0.05$ compared to saline controls. C: Representative images show aortic walls stained with hematoxylin/eosin (HE), elastica van-Gieson (EVG), or antibody against periostin at the indicated time points after application of saline or $CaCl_2$.
doi:10.1371/journal.pone.0079753.g002

in the periaortic space (**Fig. 6A**). Moreover, we found marked cellular infiltration into the rPeriostin-treated aortas (**Fig. 6A-B**). These results confirmed that periostin was sufficient for inducing *in vivo* inflammatory responses through FAK activation and MCP-1 upregulation.

Discussion

The present study demonstrated that periostin was highly expressed in human AAA, principally in the regions of cellular infiltration and elastin degradation. Periostin was also upregulated during the progression of AAA in mouse, predominantly in the phase when persistent inflammation contributed to AAA expansion. Thus, periostin showed distinct spatial and temporal expression patterns. Periostin has advantageous properties for a biomarker, because it is deposited locally in inflammatory regions, and it is also released into the circulation. Serum levels of periostin have been recognized as a potential biomarker in patients with non-small cell lung carcinoma [22] and in patients with asthma

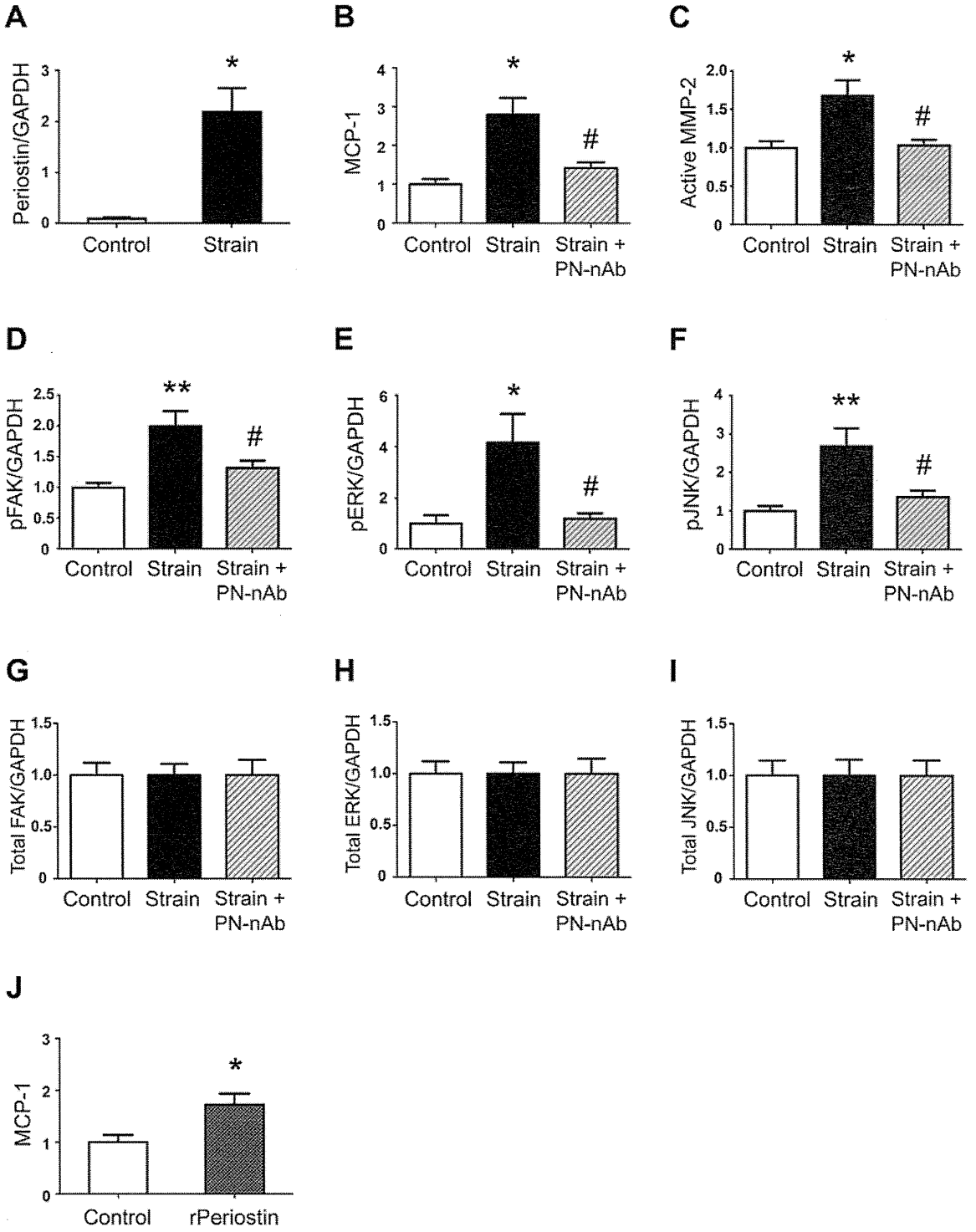

Figure 3. Role of periostin in linking mechanical strain to inflammatory responses in VSMCs. Cultured rat VSMCs treated with or without periostin-neutralizing antibody (PN-nAb, 1 μg/ml) were stimulated with cyclic uniaxial strain (20% elongation in length at a frequency of 30 cycles/min for 48 h, n = 6). Protein levels of periostin (**A**) and MCP-1 (**B**) in cell lysates were determined by western blotting. Levels of active MMP-2 in the conditioned media were determined by gelatin zymography (**C**). Levels of phosphorylated FAK (**D**), ERK (**E**) and JNK (**F**) in cell lysates were determined by western blotting. Levels of total FAK (**G**), ERK (**H**) and JNK (**I**) in cell lysates were determined by western blotting. GAPDH served as an internal control. Rat VSMCs were stimulated with recombinant periostin (rPeriostin; 1 μg/ml for 48 h; n = 4). Protein levels of MCP-1 in conditioned media were determined by ELISA (**J**). Data are mean ± SE. *$p<0.05$ and **$p<0.01$ compared to Control; #$p<0.05$ compared to VSMCs under mechanical strain.

doi:10.1371/journal.pone.0079753.g003

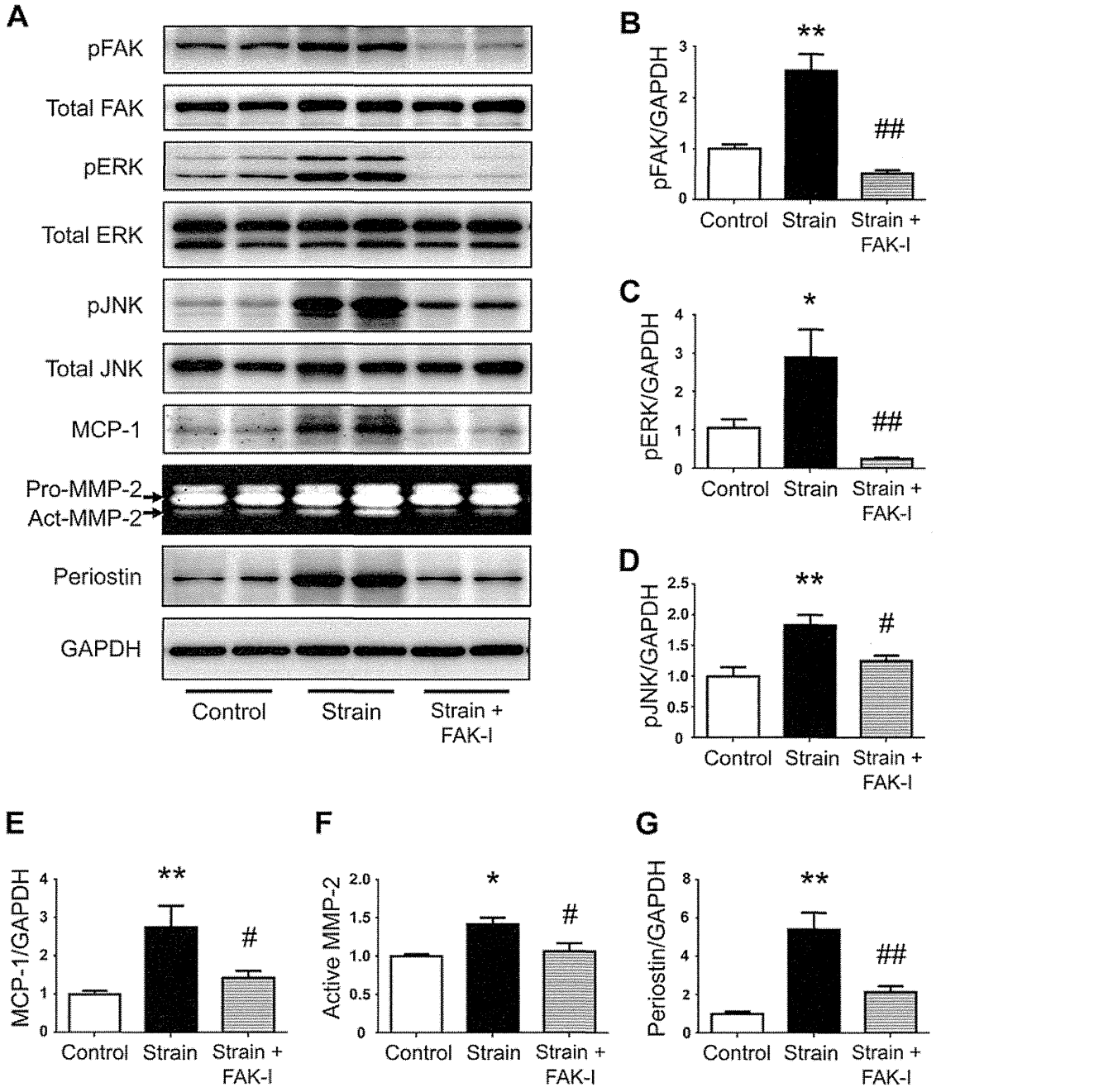

Figure 4. Role of periostin/FAK axis in mechanotransduction signaling pathway in VSMCs. Rat VSMCs were treated with or without of FAK inhibitor (PF573228, 10 μM, FAK-I) and stimulated with cyclic uniaxial strain (20% elongation in length at a frequency of 30 cycles/min for 48 h, n = 5). Levels of phosphorylated FAK (**A, B**), ERK (**A, C**) and JNK (**A, D**) in cell lysates were determined by western blotting. Protein levels of MCP-1 (**A, E**) and periostin (**A, G**) in cell lysates, and active MMP-2 (**A, F**) in conditioned media were determined by western blotting and gelatin zymography, respectively. GAPDH served as an internal control. Data are mean ± SE. *$p<0.05$ and **$p<0.01$ compared to Control; #$p<0.05$ and ##$p<0.01$ compared to VSMCs under mechanical strain.
doi:10.1371/journal.pone.0079753.g004

[23]. Thus, periostin might serve as a useful marker for detecting active stages of AAA progression.

The walls of AAA vessels are theoretically exposed to abnormally high cyclic strain, according to the Laplace law. We demonstrated that periostin was upregulated with 20% cyclic strain in VSMCs, and it was persistently increased after enlargement of the aortic diameter in AAA model mice. These data suggested that, as the aorta expands, it is exposed to pathological cyclic strain; this strain persistently upregulates periostin expression, which then accelerates AAA progression. Thus, our results suggested that periostin plays a role in AAA progression, rather than AAA initiation. In addition, we found that, when rPeriostin was implanted with Gelfoam, it did not cause destruction of elastic lamellae or the initiation of AAA in mice after 42 days (O. Yamashita and K. Yoshimura, unpublished data). Those results indicated that a transient increase in periostin was

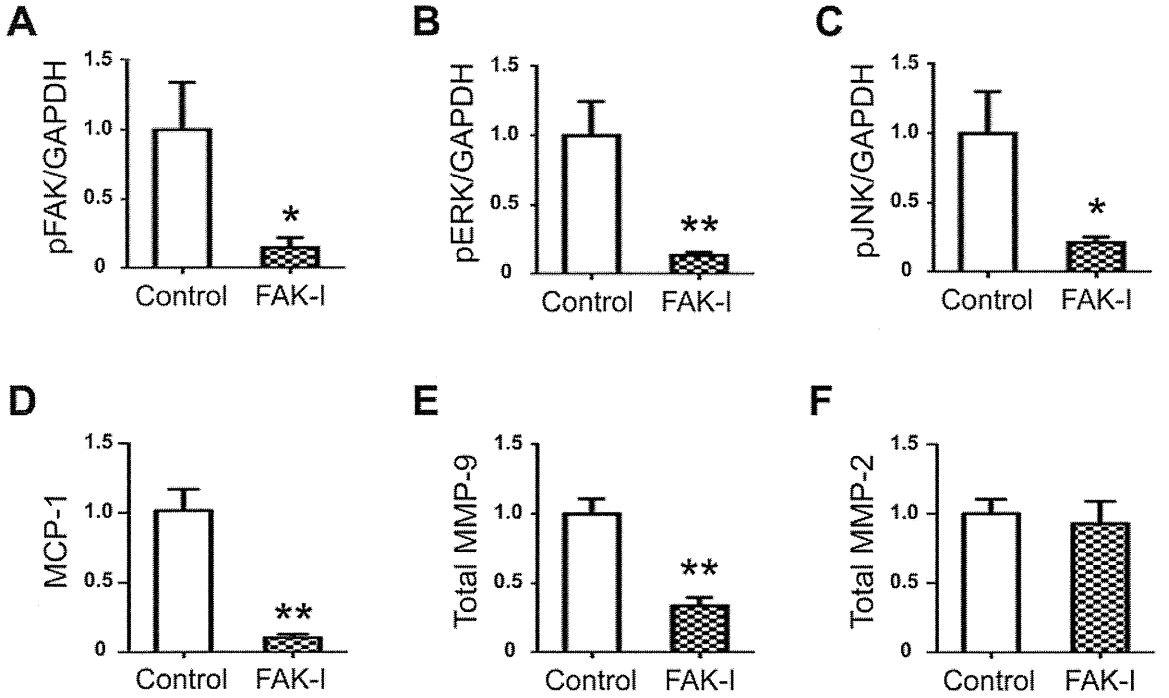

Figure 5. Role of periostin/FAK axis in sustaining inflammatory responses in human AAA tissues. Human AAA tissues were cut into small pieces and cultured with or without of FAK inhibitor (PF573228, 10 μM, FAK-I) for 48 h (n = 5). Levels of phosphorylated FAK (**A**), ERK (**B**) and JNK (**C**) in tissue lysates were determined by western blotting. GAPDH served as an internal control. Protein levels of MCP-1 (**D**) and MMPs (**E-F**) in conditioned media were determined by ELISA and gelatin zymography, respectively. Data are mean ± SE. *$p<0.05$ and **$p<0.01$ compared to Control.

doi:10.1371/journal.pone.0079753.g005

insufficient to cause the development of AAA. This data supported the notion that periostin may not play a role in the initiation of AAA.

Importantly, we also elucidated the molecular mechanism by which periostin translated mechanical strain into biochemical signals that led to inflammatory responses in AAA. Previously, several lines of evidence had suggested that mechanical stress was critical for sustaining inflammatory responses and progression in AAA. For example, clinical cohort studies revealed a positive association between hypertension and the risk of AAA [24]. In addition, it was pointed out that exclusion of AAA from systemic pressure in an endovascular aneurysm repair could lead to a reduction in the size of the AAA [25,26]. It was also reported that successful endovascular aneurysm repair caused decreases in the levels of serum interleukin-1α [27] and plasma MMP-9 [8,28]. Together, those findings implied that hemodynamic stress could contribute to aneurysm progression, both by direct physical force and by accelerating molecular biological processes. However, the molecular basis of these effects was not identified previously. To address this challenge, we examined the molecular events in VSMCs in response to cyclic strain. VSMCs are the major cells for monitoring the mechanical environment in the aortic wall [29]. Hemodynamic forces primarily include cyclic and shear stresses. The cyclic, circumferential strain, which acts perpendicular to the aortic wall, causes outward stretching of VSMCs. Fluid shear stress is the frictional force generated as blood drags against the vascular endothelial cells in the aortic wall [30]. Notably, given the same blood pressure, vessels affected by AAA will experience higher cyclic strain than normal-sized aortic vessels, according to the Laplace law. Hence, in this study, we applied supraphysiological levels of cyclic strain to VSMCs. We used 20% cyclic strain, based on previously published studies, which showed that 15% to 20% strain could be considered pathologically-elevated stretching [31–33]. On the other hand, a number of studies have used 5% to 10% cyclic strain to represent physiologically-relevant stretch conditions [33–37]. Those lower strain levels were presumably based on the observation that the maximum stretch in the human aorta during the cardiac cycle was approximately 10% under normotensive conditions [38]. Reported *in vivo* levels of aortic cyclic strain have varied widely, ranging from nearly 2% to around 20% [39–41]. This variation was probably due to differences in the methods of measurement, the ages of subjects, and the presence or absence of pathological changes. As suggested previously, pathological cyclic strain (>15%) leads to VSMC maladaptation, with enhanced growth and secretion, but physiological levels of cyclic strain maintain healthy VSMCs in a quiescent state [34,37,42]. These findings lend support to our use of 20% cyclic strain in the present study to represent pathological cyclic strain.

Crucially, our findings demonstrated for the first time that the periostin/FAK axis played a key role in maintaining and amplifying the inflammatory responses to mechanical strain in AAA (**Fig. 6C**). It was previously reported that mechanical strain caused an increase in periostin mRNA levels in Lewis lung cancer cells [10] and in periodontal ligament fibroblasts [11]. In addition, periostin was shown to be essential for activation of FAK in VSMCs [16] and in cardiac cells [17]. More recently, it was reported that mechanical stress, though not a cyclic strain, caused FAK activation and promoted MCP-1 secretion through the FAK/ERK pathway in the pathological mechanisms of skin fibrosis [18]. In addition, MMP-2 and MMP-9 were reported to be upregulated by periostin in cardiac cells [12], and also by FAK activation in a fibroblast cell line [43]. Here, we integrated these findings and successfully demonstrated the involvement of the periostin/FAK axis in mechanotransduction in VSMCs. Surpris-

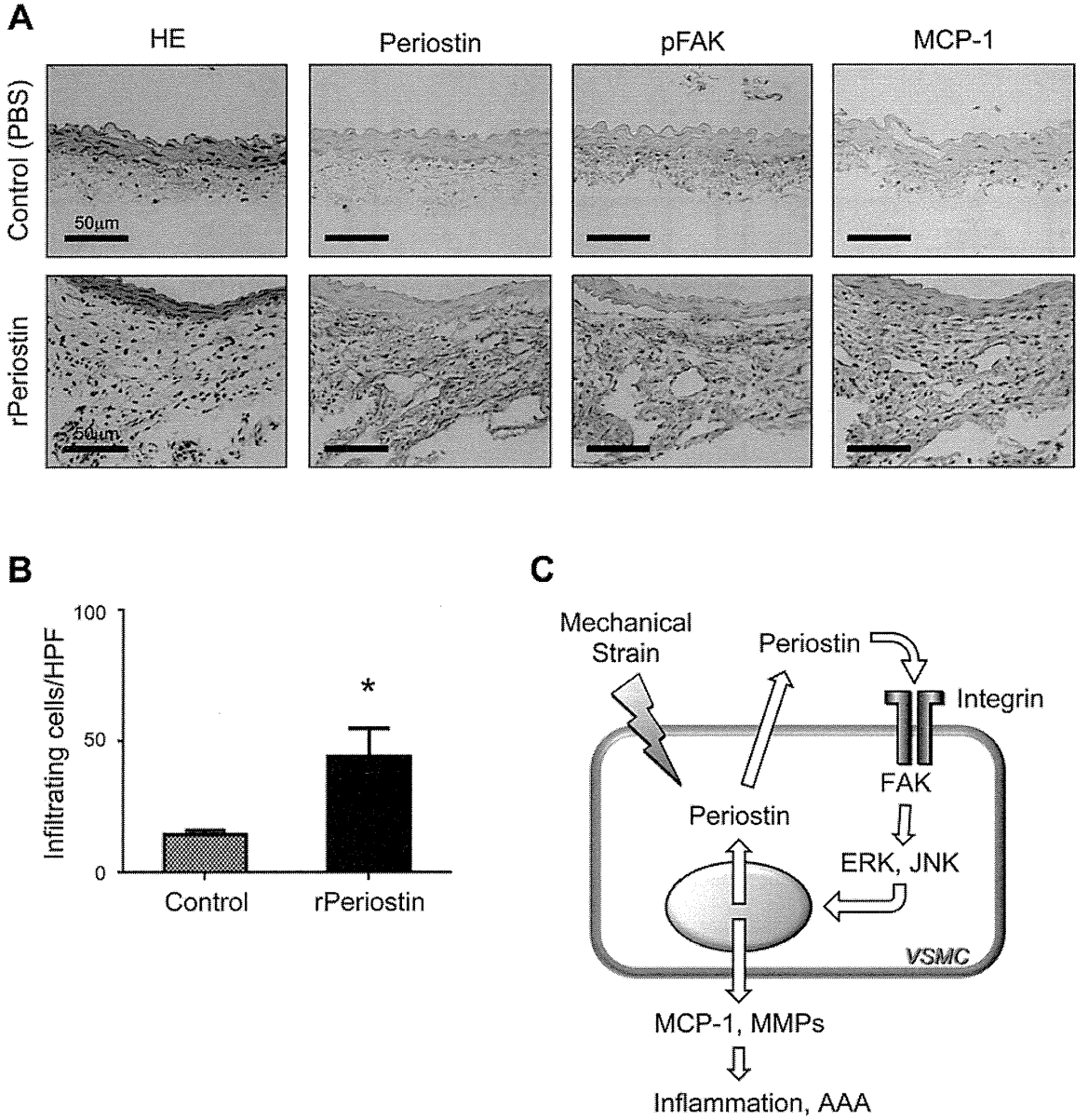

Figure 6. Role of periostin in inducing inflammatory responses *in vivo*. **A-B**: Gelfoam patches containing PBS (Control, n = 6) or recombinant periostin (rPeriostin, n = 7) were placed into periaortic spaces of mice for 7 days. Representative images show mouse aortic walls, stained with hematoxylin/eosin (HE) or with antibodies against periostin, phosphorylated FAK (pFAK), or MCP-1 (**A**). Infiltrating cells were counted in 5-10 high-power fields (**B**). Data are mean ± SE. *$p<0.05$ compared to Control. **C**: Schematic diagram represents the proposed vicious cycle of periostin upregulation driven by mechanical strain through activation of FAK, resulting in the maintenance of inflammation in AAA.
doi:10.1371/journal.pone.0079753.g006

ingly, we also discovered a vicious cycle between periostin production and FAK activation in VSMCs. We found that inhibition of either periostin or FAK resulted in suppression of both proteins. In human AAA tissues, we observed upregulation of periostin and significant activation of FAK. We also showed that inhibition of FAK dramatically decreased the activation of JNK. We previously found that secretion of periostin was significantly diminished with a JNK inhibitor, SP600125, in *ex vivo* human AAA tissue cultures (K. Yoshimura, unpublished data). Taken together, these findings strongly suggested that a vicious cycle among periostin, FAK, and JNK could amplify the inflammatory responses to mechanical strain in human AAA. Thus, our results suggested that relentless pathological strain on AAA walls leads to continuous activation of the periostin/FAK axis, thereby causing sustained upregulation of MCP-1 and MMPs, and finally resulting in progression of AAA. Indeed, our results showed that application of periostin in mouse aortic walls activated FAK and upregulated MCP-1, which resulted in cellular infiltration. It was previously known that MCP-1 and MMPs were highly upregulated in the walls of human AAA specimens [13,44]; in addition, these molecules also played critical roles in inflammatory cell infiltration and extracellular matrix degradation during the development of AAA in mice [45,46]. We previously reported that JNK played an essential role in abnormal extracellular matrix metabolism and disease progression in AAA. We also showed that inhibition of JNK prevented the development of AAA and could also cause

regression of established AAA in mice [13]. Hence, JNK is a key molecule in the pathogenesis of AAA. In the current work, we showed that JNK was also involved in the vicious cycle of periostin upregulation, driven by mechanical strain, during the progression of AAA.

In conclusion, this study provided new insights into the underlying mechanisms that link periostin to mechanical strain and inflammation in the progression of AAA. Our findings revealed a novel vicious cycle, which is driven by mechanical strain, and leads to the amplification and maintenance of inflammatory responses. Thus, periostin may represent both a clinical biomarker for disease activity in AAA and a therapeutic target for patients with AAA.

References

1. Sakalihasan N, Limet R, Defawe OD (2005) Abdominal aortic aneurysm. The Lancet 365: 1577–1589.
2. Yoshimura K, Aoki H (2012) Recent advances in pharmacotherapy development for abdominal aortic aneurysm. Int J Vasc Med 2012: 648167.
3. Rooke TW, Hirsch AT, Misra S, Sidawy AN, Beckman JA, et al. (2011) 2011 ACCF/AHA Focused Update of the Guideline for the Management of patients with peripheral artery disease (Updating the 2005 Guideline): a report of the American College of Cardiology Foundation/American Heart Association Task Force on practice guidelines. Circulation 124: 2020–2045.
4. Golledge J, Muller J, Daugherty A, Norman P (2006) Abdominal aortic aneurysm: pathogenesis and implications for management. Arterioscler Thromb Vasc Biol 26: 2605–2613.
5. Golledge J, Powell JT (2007) Medical management of abdominal aortic aneurysm. Eur J Vasc Endovasc Surg 34: 267–273.
6. Thompson RW, Geraghty PJ, Lee JK (2002) Abdominal aortic aneurysms: basic mechanisms and clinical implications. Curr Probl Surg 39: 110–230.
7. Tedesco MM, Dalman RL (2010) Arterial Aneurysms. In: Cronenwett JL, Johnston KW, editors. Vascular Surgery. Philadelphia: Saunders. pp. 117–130.
8. Sangiorgi G, D'Averio R, Mauriello A, Bondio M, Pontillo M, et al. (2001) Plasma Levels of Metalloproteinases-3 and -9 as Markers of Successful Abdominal Aortic Aneurysm Exclusion After Endovascular Graft Treatment. Circulation 104: I-288-I-295.
9. Kudo A (2011) Periostin in fibrillogenesis for tissue regeneration: periostin actions inside and outside the cell. Cell Mol Life Sci 68: 3201–3207.
10. Ma D, Lu H, Xu L, Xu X, Xiao W (2009) Mechanical loading promotes Lewis lung cancer cell growth through periostin. In Vitro Cell Dev Biol Anim 45: 467–472.
11. Wen W, Chau E, Jackson-Boeters L, Elliott C, Daley TD, et al. (2010) TGF-beta1 and FAK regulate periostin expression in PDL fibroblasts. J Dent Res 89: 1439–1443.
12. Hakuno D, Kimura N, Yoshioka M, Mukai M, Kimura T, et al. (2010) Periostin advances atherosclerotic and rheumatic cardiac valve degeneration by inducing angiogenesis and MMP production in humans and rodents. J Clin Invest 120: 2292–2306.
13. Yoshimura K, Aoki H, Ikeda Y, Fujii K, Akiyama N, et al. (2005) Regression of abdominal aortic aneurysm by inhibition of c-Jun N-terminal kinase. Nat Med 11: 1330–1338.
14. Nagasawa A, Yoshimura K, Suzuki R, Mikamo A, Yamashita O, et al. (2013) Important role of the angiotensin II pathway in producing matrix metalloproteinase-9 in human thoracic aortic aneurysms. J Surg Res.
15. Kimura T, Yoshimura K, Aoki H, Imanaka-Yoshida K, Yoshida T, et al. (2011) Tenascin-C is expressed in abdominal aortic aneurysm tissue with an active degradation process. Pathology International 61: 559–564.
16. Li G, Jin R, Norris RA, Zhang L, Yu S, et al. (2010) Periostin mediates vascular smooth muscle cell migration through the integrins alphavbeta3 and alphavbeta5 and focal adhesion kinase (FAK) pathway. Atherosclerosis 208: 358–365.
17. Shimazaki M, Nakamura K, Kii I, Kashima T, Amizuka N, et al. (2008) Periostin is essential for cardiac healing after acute myocardial infarction. J Exp Med 205: 295–303.
18. Wong VW, Rustad KC, Akaishi S, Sorkin M, Glotzbach JP, et al. (2012) Focal adhesion kinase links mechanical force to skin fibrosis via inflammatory signaling. Nat Med 18: 148–152.
19. Yoshimura K, Aoki H, Ikeda Y, Furutani A, Hamano K, et al. (2008) Development of pharmacological therapy for abdominal aortic aneurysms based on animal studies. In: Sakalihasan N, editor. Aortic Aneurysms, New insights into an old problem. Liège: Édition de l'Université de Liège.
20. Walton LJ, Franklin IJ, Bayston T, Brown LC, Greenhalgh RM, et al. (1999) Inhibition of prostaglandin E2 synthesis in abdominal aortic aneurysms: implications for smooth muscle cell viability, inflammatory processes, and the expansion of abdominal aortic aneurysms. Circulation 100: 48–54.
21. Kuhn B, del Monte F, Hajjar RJ, Chang YS, Lebeche D, et al. (2007) Periostin induces proliferation of differentiated cardiomyocytes and promotes cardiac repair. Nat Med 13: 962–969.
22. Sasaki H, Dai M, Auclair D, Fukai I, Kiriyama M, et al. (2001) Serum level of the periostin, a homologue of an insect cell adhesion molecule, as a prognostic marker in nonsmall cell lung carcinomas. Cancer 92: 843–848.
23. Jia G, Erickson RW, Choy DF, Mosesova S, Wu LC, et al. (2012) Periostin is a systemic biomarker of eosinophilic airway inflammation in asthmatic patients. J Allergy Clin Immunol 130: 647–654 e610.
24. Chaikof EL, Brewster DC, Dalman RL, Makaroun MS, Illig KA, et al. (2009) The care of patients with an abdominal aortic aneurysm: the Society for Vascular Surgery practice guidelines. J Vasc Surg 50: S2–49.
25. Ellozy SH, Carroccio A, Lookstein RA, Jacobs TS, Addis MD, et al. (2006) Abdominal aortic aneurysm sac shrinkage after endovascular aneurysm repair: correlation with chronic sac pressure measurement. J Vasc Surg 43: 2–7.
26. Kwon ST, Rectenwald JE, Baek S (2011) Intrasac pressure changes and vascular remodeling after endovascular repair of abdominal aortic aneurysms: review and biomechanical model simulation. J Biomech Eng 133: 011011.
27. Yates CM, Abdelhamid M, Adam DJ, Nash GB, Bradbury AW, et al. (2011) Endovascular aneurysm repair reverses the increased titer and the inflammatory activity of interleukin-1alpha in the serum of patients with abdominal aortic aneurysm. J Vasc Surg 54: 497–503.
28. Hellenthal FA, Ten Bosch JA, Pulinx B, Wodzig WK, de Haan MW, et al. (2012) Plasma levels of matrix metalloproteinase-9: a possible diagnostic marker of successful endovascular aneurysm repair. Eur J Vasc Endovasc Surg 43: 171–172.
29. Feng Y, Yang JH, Huang H, Kennedy SP, Turi TG, et al. (1999) Transcriptional profile of mechanically induced genes in human vascular smooth muscle cells. Circ Res 85: 1118–1123.
30. Cummins PM, von Offenberg Sweeney N, Killeen MT, Birney YA, Redmond EM, et al. (2007) Cyclic strain-mediated matrix metalloproteinase regulation within the vascular endothelium: a force to be reckoned with. Am J Physiol Heart Circ Physiol 292: H28–42.
31. Cattaruzza M, Dimigen C, Ehrenreich H, Hecker M (2000) Stretch-induced endothelin B receptor-mediated apoptosis in vascular smooth muscle cells. FASEB J 14: 991–998.
32. Nguyen KT, Frye SR, Eskin SG, Patterson C, Runge MS, et al. (2001) Cyclic strain increases protease-activated receptor-1 expression in vascular smooth muscle cells. Hypertension 38: 1038–1043.
33. Qi YX, Qu MJ, Yan ZQ, Zhao D, Jiang XH, et al. (2010) Cyclic strain modulates migration and proliferation of vascular smooth muscle cells via Rho-GDIalpha, Rac1, and p38 pathway. J Cell Biochem 109: 906–914.
34. Chapman GB, Durante W, Hellums JD, Schafer AI (2000) Physiological cyclic stretch causes cell cycle arrest in cultured vascular smooth muscle cells. Am J Physiol Heart Circ Physiol 278: H748–754.
35. Asanuma K, Magid R, Johnson C, Nerem RM, Galis ZS (2003) Uniaxial strain upregulates matrix-degrading enzymes produced by human vascular smooth muscle cells. Am J Physiol Heart Circ Physiol 284: H1778–1784.
36. Morrow D, Sweeney C, Birney YA, Cummins PM, Walls D, et al. (2005) Cyclic strain inhibits Notch receptor signaling in vascular smooth muscle cells in vitro. Circ Res 96: 567–575.
37. Kona S, Chellamuthu P, Xu H, Hills SR, Nguyen KT (2009) Effects of cyclic strain and growth factors on vascular smooth muscle cell responses. Open Biomed Eng J 3: 28–38.
38. Dobrin PB (1978) Mechanical properties of arterises. Physiol Rev 58: 397–460.
39. Faries PL, Agarwal G, Lookstein R, Bernheim JW, Cayne NS, et al. (2003) Use of cine magnetic resonance angiography in quantifying aneurysm pulsatility associated with endoleak. J Vasc Surg 38: 652–656.
40. van Keulen JW, van Prehn J, Prokop M, Moll FL, van Herwaarden JA (2009) Dynamics of the aorta before and after endovascular aneurysm repair: a systematic review. Eur J Vasc Endovasc Surg 38: 586–596.
41. Goergen CJ, Barr KN, Huynh DT, Eastham-Anderson JR, Choi G, et al. (2010) In vivo quantification of murine aortic cyclic strain, motion, and curvature:

Acknowledgments

We thank M. Oishi (Yamaguchi University, Japan) and S. Nishino-Fujimoto (Yamaguchi University, Japan) for technical assistance. Most of the culture and animal experiments were performed at the Science Research Center, Yamaguchi University.

Author Contributions

Conceived and designed the experiments: KY. Performed the experiments: OY. Analyzed the data: OY AN KU. Contributed reagents/materials/analysis tools: YI NM KH. Wrote the paper: KY OY.

implications for abdominal aortic aneurysm growth. J Magn Reson Imaging 32: 847–858.
42. Williams B (1998) Mechanical influences on vascular smooth muscle cell function. J Hypertens 16: 1921–1929.
43. Sein TT, Thant AA, Hiraiwa Y, Amin AR, Sohara Y, et al. (2000) A role for FAK in the Concanavalin A-dependent secretion of matrix metalloproteinase-2 and -9. Oncogene 19: 5539–5542.
44. Kudo J, Yoshimura K, Hamano K (2007) Simvastatin reduces secretion of monocyte chemoattractant proteins and matrix metalloproteinase-9 in human abdominal aortic aneurysms. Bull Yamaguchi Med School 54: 47–56.
45. Ishibashi M (2004) Bone Marrow-Derived Monocyte Chemoattractant Protein-1 Receptor CCR2 Is Critical in Angiotensin II-Induced Acceleration of Atherosclerosis and Aneurysm Formation in Hypercholesterolemic Mice. Arteriosclerosis, Thrombosis, and Vascular Biology 24: e174–e178.
46. Longo GM, Xiong W, Greiner TC, Zhao Y, Fiotti N, et al. (2002) Matrix metalloproteinases 2 and 9 work in concert to produce aortic aneurysms. J Clin Invest 110: 625–632.

Flying with giant coronary aneurysms caused by Kawasaki disease

Yozo Teramachi [a], Kenji Suda [a,*], Shunich Ogawa [b], Hiroshi Kamiyama [c], Kenji Hamaoka [d]

[a] Department of Pediatrics and Child Health, Kurume University School of Medicine, Japan
[b] Department of Pediatrics, Nippon Medical School, Japan
[c] Department of Pediatrics, Nihon University School of Medicine, Japan
[d] Department of Pediatrics, Kyoto Prefectural Medical University, Japan

ARTICLE INFO

Article history:
Received 8 July 2013
Accepted 13 July 2013
Available online 2 August 2013

Keywords:
Kawasaki disease
Giant coronary aneuryms
Air flight
Cardiac event

Kawasaki disease (KD) is the most prevalent vasculitis in the developed countries and can leave giant coronary artery aneurysms (gCAA) even with recommended treatment including intravenous immunoglobulin infusion. These patients with gCAA carry a risk of acute thrombosis leading to myocardial infarction and are frequently placed on thromboprophylaxis including warfarin and aspirin [1].

Air travel is known to increase coagulation activity [2] and leads to venous thrombosis, known as "Economy class syndrome", and occasionally to systemic arterial thrombosis [3,4]. However, there is no data available concerning safety of air travel in these patients with gCAA caused by KD and therefore we conducted this multi-institutional study.

We arbitrarily chose 4 institutions that have treated many patients with gCAA caused by KD in Japan and sent questionnaires to ask if there were any patients with gCAA who had traveled by air and, if so, patients' demographic characteristics including sex, maximum size of gCAA, site of gCAA, age at air travel, number of air travel, flight time, medication at flight, pre-flight international normalized ratio of prothrombin time in those with warfarin administration, any cardiac event, and age at the final visit.

In total, 16 patients (13 male) with gCAA had 53 air trips (50 round and 3 one-way trip), but no patient has experienced any cardiac event (Table 1). GCAA was 14.7 ± 7.0 (8–33) mm in diameter and was at left coronary artery in 9, both left and right coronary arteries in 5, and right coronary artery in 2. The age at air travel was 8.8 ± 4.8 (range 0.6–21) years old, 6.1 ± 4.7 (0–20.2) years after the onset of KD. The median number of air trips was 1 (1–22) for each patient. Flight time ranged from 1.5 to 13 h and was <3 h in 48 (91%), but was ≥10 hours in 4. The purpose of the flight was mainly regular hospital visit or vacation (n = 46), and was occasionally surgical (n = 6) or for catheter intervention (n = 1) for myocardial ischemia.

During the flight, patients were placed on warfarin in 35 (66%) air trips with 1.6 ± 0.7 (0.9–3.6) of PT-INR, on single or double antiplatelet drugs without warfarin in 16. Patient 4 had the remaining 2 flights, 13 h and 1.5 h, without thromboprophylaxis, in that he traveled without knowing about a gCAA in the acute phase and had been placed on prednisolone. He was placed on warfarin in the subsequent air flights. Patients 2, 3, and 13, had 14 air trips with aspirin alone without warfarin for regular hospital visit.

Of note, 2 patients with gCAA and coronary stenosis ≥90% without warfarin had air travel without a cardiac event. Patient 15 had 90% stenosis at segment 6 and flew from Indonesia to Japan, a

Table 1

#	Age at onset (y.o.)	Sex	# of flight	Segments of GA	Maximum size of GA (mm)	Age at flight (y.o.)	Flight time (h)	Medications	Target PT-INR	PT-INR before flight	Final follow up (y.o.)	Comments
1	1.8	M	23	5	9.8	3.0–17.0	2 × 22 3 × 1 1.5 × 6	Wa, ASA, DP	2.5	2.2	19.1	
2	5.5	M	9	6	9.4	8.0–17.0	2 × 3	ASA	–	–	22.2	
3	0.7	M	4	1, 2	8	1.0–10.1	2	ASA	–	–	30.5	
4	0.6	M	3	1, 2	11	0.6, 0.6, 1.2	13, 1.5, 2	Predonisolone Wa, ASA, Enalapril,	–	–	6.5	Traveled w/o knowing gCAA
5	1.5	M	2	5	14.2	4.0, 7.0	1.5, 3	Wa, ASA, TP	2.5	1.74	8.0	
6	5.6	M	2	1–2, 5–6–7	24	7.6, 8.2	3 × 2	Wa, ASA	2.5–3.5	3.62	7.6	
7	3.5	M	1	1–2, 6–7	33	6.1	1.5	Wa, ASA	2.5–3.0	2.8	6.1	
8	3.1	M	1	5, 6	11.1	7.2	2	Wa, ASA	2.0–2.5			
9	3.8	M	1	1–2, 5–6	18	8.4	2	Wa, ASA	2.0–2.5	1.62	9.4	
10	10.4	M	1	1–2, 5–6	22.3	10.8	2	Wa, ASA	2.0–2.5	2.3	10.9	
11	1.5	M	1	5–6	13	17.0	13	Wa, ASA	2.0–2.5	2.1	23.1	
12	0.6	F	1	6	10	19.0	12	ASA, Wa, Statin	2	1.8	19.0	
13	0.8	M	1	6	9	21.0	6	ASA, Wa, Statin	2	1.6	21.0	
14	0.8	M	1	1, 5	20	16.0	2	ASA	–	–	23.5	
15	6.5	F	1	6	10.5	13.1	10	ASA			13.1	90% stenosis at segment 6
16	2.6	F	1	5	11.6	6.8	2	ASA, DP, propranolol	–	–	25.2	≧90% stenosis at both coronary arteries

Abbreviations.
ASA, aspirin; DP, dipyridamole; F, female; GA, giant coronary aneurysm; M, male; PT-INR, International normalized ratio for prothrombin time; Wa, warfarin; y.o., years old.

* Corresponding author at: Department of Pediatrics and Child Health, Kurume University School of Medicine, Asahi-Machi 67, Kurume, 830-0011, Japan. Tel.: +81 942 31 7565; fax: +81 942 38 1792.
E-mail address: suda_kenji@med.kurume-u.ac.jp (K. Suda).

10 h flight, with only aspirin, to have successful surgical intervention. Patient 16 had ≥90% stenosis at both coronary arteries and had air travel with aspirin, dipyridamole, and propranolol to get a second opinion. Later she underwent catheter and surgical intervention for myocardial ischemia. All patients survived until 16.3 ± 7.9 (6.1–30.5) years old as the latest follow-up.

This study indicates that, though there is a theoretical risk of cardiac events in patients with gCAA during or after air travel, they can travel safely using air flights up to 3 h with standard thromboprophylaxis using either warfarin or aspirin. Indeed, there was no single episode of cardiac event in this study.

One of the factors should be flight time that might have significant impact on coronary thrombus formation. Concerning venous thromboembolism, a dose–response relationship was observed, with a 26% higher risk for every 2 h of air travel [5]. As to systemic arterial thrombosis, we have seen a patient with cyanotic congenital heart disease who suffered from obstruction of an arterial shunt after 8 h of flight [3]. Also Liang et al. reported a 37 year-old woman who suffered from acute myocardial infarction after a 12-h flight, from the United States to Taiwan [4]. Because most (91%) of the flight times in this study were <3 h, we may not extrapolate our observation to the longer flights. Further data concerning longer flight experience must be accumulated.

Another factor should be thromboprophylaxis such as warfarin and anti-platelet agents. It is hard to comment on the safety of air travel without warfarin in patients with gCAA because we have only 16 air flights without warfarin in 5 patients.

In conclusion, though there is a theoretical risk of a cardiac event in patients with gCAA during or after air travel, they may fly safely up to 3 h without significant risk. Further study including longer flight is necessary.

References

[1] Suda K, Kudo Y, Higaki T, et al. Multicenter and retrospective case study of warfarin and aspirin combination therapy in patients with giant coronary aneurysms caused by Kawasaki disease. Circ J 2009;73:1319–23.
[2] Schreijer AJ, Cannegieter SC, Meijers JC, Middeldorp S, Büller HR, Rosendaal FR. Activation of coagulation system during air travel: a crossover study. Lancet 11 2006;367:832–8.
[3] Suda K, Matsumura M, Matsumoto M. Shunt obstruction after an air travel in an adult patient with cyanotic congenital heart disease. Cardiology 2005;103:142.
[4] Liang HY, Lin CC, Lee CS, Chen YF, Hwang YS. Acute myocardial infarction with patent coronary artery after a long-distance flight-a case report. Kaohsiung J Med Sci 2002;18:35–8.
[5] Chandra D, Parisini E, Mozaffarian D. Meta-analysis: travel and risk for venous thromboembolism. Ann Intern Med 2009;151:180–90.

0167-5273/$ – see front matter
http://dx.doi.org/10.1016/j.ijcard.2013.07.141

PEDIATRICS INTERNATIONAL Official Journal of the Japan Pediatric Society

Pediatrics International (2013) **55**, 690–695 doi: 10.1111/ped.12187

Original Article

National Japanese survey of thrombolytic therapy selection for coronary aneurysm: Intracoronary thrombolysis or intravenous coronary thrombolysis in patients with Kawasaki disease

Mana Harada,[1] Katsumi Akimoto,[1] Shunichi Ogawa,[2] Hitoshi Kato,[3] Yosikazu Nakamura,[6] Kenji Hamaoka,[7] Tsutomu Saji,[4] Toshiaki Shimizu[1] and Tatsuo Kato[5]

[1]*Department of Pediatrics, Juntendo University Faculty of Medicine,* [2]*Department of Pediatrics, Nippon Medical School,* [3]*Department of Cardiovascular Medicine, National Center for Child Health and Development,* [4]*First Department of Pediatrics, Toho University,* [5]*Cardiovascular Medicine, National Research Institute for Child Health and Development, Tokyo,* [6]*Department of Public Health, Jichi Medical University, Tochigi, and* [7]*Department of Pediatric Cardiology and Nephrology, Graduate School of Medicine, Kyoto Prefectural University of Medicine, Kyoto, Japan*

Abstract ***Background***: Thrombolytic therapy for coronary aneurysm thrombosis of Kawasaki disease (KD) includes antiplatelet and anticoagulants, i.v. coronary thrombolysis (IVCT), and i.c. thrombolysis (ICT). Therapeutic methods, drugs and doses vary among medical facilities.

Methods and Results: A nationwide survey of thrombolytic therapy was conducted under the auspices of the Ministry of Health, Labour and Welfare Research Program to Intractable Diseases Research Grants. A secondary survey targeted 14 facilities conducting thrombolytic therapy during a 5 year period (2004–2009). The primary survey investigated performance of thrombolytic therapy for 23 KD patients at 14 facilities, and of these, five with acute myocardial infarction had received ICT and combined therapy. The secondary survey investigated the pre-treatment condition of aneurysm and thrombosis and actual treatment methods. ICT was effective for small thrombi (≤10 mm), while IVCT was effective even for giant thrombi (>10 mm). ICT was also effective for thrombi within several hours after formation.

Conclusion: In the present nationwide survey, thrombolytic therapy was more effective in cases of a shorter duration between thrombus formation and the start of treatment. It was found that many facilities used only IVCT for thrombus alone. Medications given to KD children did not cause serious hemorrhagic complications, unlike in adults. Although doses exceeded recommended levels in many cases, the only complications were nasal bleeding and fever.

Key words acute myocardial infarction, coronary aneurysm, coronary thrombolysis, i.c. thrombolysis, Kawasaki disease.

Kawasaki disease (KD) is an unexplained vasculitis affecting medium-sized and small blood vessels in infants and children under the age of 5 years. With the wide availability of immunoglobulin therapy for this disease, the incidence of coronary aneurysm in KD patients has decreased but still reportedly ranges from 3% to 10%. In KD patients with giant coronary aneurysms, thrombus formation is occasionally seen despite the use of antithrombotic agents.[1,2] During the acute through recovery phases of KD, coronary aneurysms can form as a result of vascular remodeling associated with vasculitis. Coronary aneurysm formation can, in turn, trigger not only hemodynamic changes but also dysfunction of vascular endothelial cells, inducing potentially fatal thrombus formation and myocardial ischemia.[3] Within a giant aneurysm, among other features, shear stress is lower than normal, often resulting in thrombus formation (primarily fibrin thrombi) due to activation of clotting factors.[4,5] Fresh floating thrombi within the aneurysm require particularly careful follow up because they can cause acute myocardial infarction (AMI).

Thrombi can be divided into two types: venous (primarily fibrin thrombus) and arterial (platelet thrombus arising from atherosclerosis). Fibrin thrombi are a major type of thrombus formed in KD patients. Therefore, the methods for prevention and treatment of this type of thrombus differ from those for thrombi generally seen in adults, that is, thrombi arising from collapse of atheromatous plaques following progression of atherosclerosis.[6]

I.v. coronary thrombolysis (IVCT) involves heparin, urokinase, and tissue-type plasminogen activator (t-PA).[7] t-PA is an established means of treating AMI in adults. Under the national health insurance system of Japan, the use of t-PA, in addition to urokinase, has been partially authorized for i.c. thrombolysis (ICT) in adult cases.[8–11] To date, however, there has been little clinical experience with the use of t-PA for ICT in children with KD. Because a high incidence of hemorrhagic complications arising from thrombolytic therapy has been recognized as a

Correspondence: Mana Harada, MD, 7-4-811 Ichigayahonmura-cho, Shinjuku-ku, 162-0845, Tokyo, Japan. Email: mana_mimana@yahoo.co.jp

Received 3 April 2012; revised 13 August 2012; accepted 24 June 2013.

problem and because IVCT with t-PA has been reported to have similar efficacy to that of t-PA used for ICT, only urokinase has been authorized for ICT in children, while pediatric use of t-PA for ICT is not reimbursed under the health insurance system of Japan.[11] In practice, however, t-PA has frequently been used for ICT of coronary aneurysm thrombosis with KD in many facilities.

Thus, there are many open questions related to the efficacy of drugs and treatment methods (e.g. IVCT and ICT) selected for thrombolysis. Although existing guidelines refer to selection of drugs and treatment methods, the drugs and methods actually selected vary among facilities.

Methods

The Study Group for Preparing Guidelines for Therapy for Refractory Kawasaki Disease, organized within the framework of the Ministry of Health, Labour and Welfare Research Program for Intractable Diseases Research Grants, conducted a nationwide survey in Japan on coronary aneurysm thrombolytic therapy, primarily using documents, postal mailing, email, and telephone communication. The primary survey pertained to experience with thrombolytic therapy and development of AMI at individual facilities. Primary surveys were given to 498 pediatric departments throughout Japan. Of these 498 facilities, 14 had carried out thrombolytic therapy during a 5 year period (2004–2009). The secondary survey was carried out at these 14 facilities.

The secondary survey pertained to the gender and age of the patients receiving thrombolytic therapy, their clinical status before the start of treatment (whether they had thrombi alone or also AMI), estimated length of time after thrombus formation (estimated length of time from thrombus formation until detection and onset of AMI), and size and location of aneurysms and thrombi. The survey was additionally designed to investigate the method used for thrombolytic therapy (IVCT, ICT, or combined therapy), drugs used (urokinase, t-PA, urokinase + t-PA etc.), frequency and duration of treatment, presence/absence of complications associated with therapy, and thrombolytic effects. The endpoints in the evaluation of thrombolytic effects were established as follows: ICT is a therapy in which a thrombus in the coronary aneurysm is directly injected with an anti-thrombotic drug. Successful thrombolysis can be achieved by ICT and generally confirmed if the thrombus has been dissolved immediately after treatment. Thrombolytic effects beyond this do not depend on the ICT technique itself; therefore, they should be distinguished from the effects of IVCT. There is no set evaluation time limit; therefore, the endpoint of the ICT thrombolysis evaluation was set at 6 h. According to the nationwide survey results, thrombolytic effects were achieved approximately12–96 h after the initiation or completion of IVCT; therefore, the endpoint was set at 3 days, and an evaluation of the effects of thrombolytic therapy was performed. The judgment 'effective' was made in cases in which echocardiography and coronary angiography confirmed thrombi to have disappeared or regressed, accompanied by improved blood flow.

In one case in which combined therapy was conducted immediately following ICT, no change in the thrombus size was observed on coronary angiography or subsequent echocardiography. After approximately 5 h of ICT, IVCT was initiated. On day 2 of IVCT, a reduction in the thrombus size was confirmed via echocardiography. Here ICT was judged as 'not effective' and IVCT as 'effective'.

Results

At the 14 facilities selected on the basis of the primary survey results, thrombolytic therapy had been carried out on 23 patients in total. When responses of these 23 patients to therapy were evaluated for each therapeutic method, a response (thrombolytic effect) was seen in nine (75%) of the 12 patients receiving IVCT, four (66.7%) of the six receiving ICT, and three (60%) of the five receiving a combination of IVCT and ICT. Of the 23 patients, five developed AMI, and all five had received ICT (independently or in combination with IVCT), that is, none had received only IVCT.

Figure 1 shows patient clinical status (i.e. thrombus alone or complicated by AMI) before the start of thrombolytic therapy. Of the five patients with AMI, four received ICT alone and one received combined therapy. Among the four patients receiving ICT alone, two had thrombolysis and improved blood flow, that is, good response to therapy. The patient receiving combined therapy had neither thrombolysis nor improved blood flow, when rated using the current criteria for efficacy evaluation. There were 18 asymptomatic patients in whom only thrombus formation was detected. As to selection of treatment methods and responses to therapy in these 18 patients, response was noted in nine (75%) of the 12 receiving IVCT alone, one (50%) of the two receiving ICT alone, and two (50%) of the four receiving combined therapy.

In the secondary survey aimed at gathering more detailed information, responses were obtained from 11 of the 14 facilities, allowing collection of detailed information on thrombolytic therapy for 20 patients in total. These 20 patients consisted of 17 male and three females subjects, ranging in age from 4 months to 25 years (mean, 3 years 5 months). More than half of the 20 patients were ≤2 years of age, and most were boys (81.8%).

The average vertical diameter of the coronary aneurysm that formed thrombi was 10.5 mm (range, 6.0–15.0 mm) in the left coronary artery and 9.5 mm (range, 8.0–20.0 mm) in the right coronary artery. Figure 2 shows the data on response to each treatment method, analyzed by thrombus size. Thrombus size was defined as the maximum diameter in a direction perpendicular to the course of the coronary artery. ICT was particularly effective for small thrombi, that is, ≤10 mm, while IVCT was effective even for giant thrombi (>10 mm).

Figure 3 shows treatment response in relation to the estimated length of time from thrombus formation until the start of treatment. According to the ACC/AHA guidelines, thrombolytic therapy is indicated within 12 h after the onset of AMI. In patients without symptoms of AMI, however, in whom only a thrombus within the coronary aneurysm has been detected, it is rare for precise information to be available regarding the time of thrombus formation, that is, the time elapsed since thrombus formation. With this in mind, we analyzed treatment response by

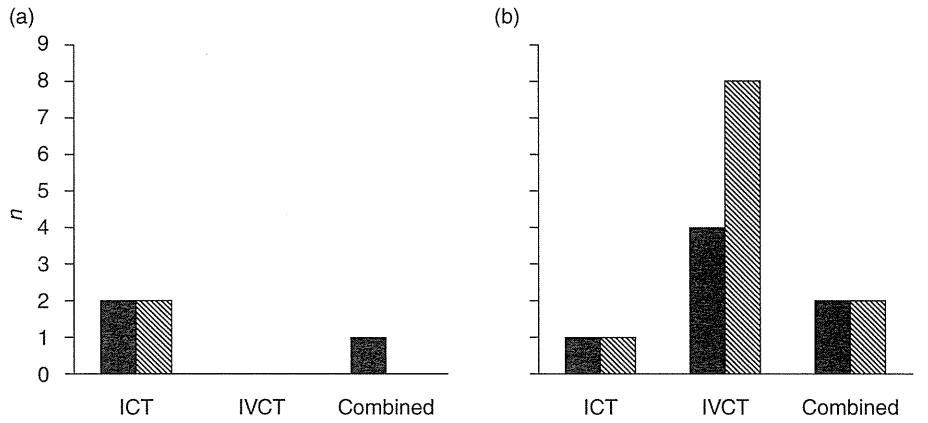

Fig. 1 Patient clinical status before the start of thrombolytic therapy: (a) acute myocardial infarction (AMI; $n = 5$); (b) asymptomatic (i.e. thrombus alone; $n = 18$). The 23 patients managed at 14 facilities, and selected on the basis of the primary survey results, were divided into two groups (a, b) and their treatment response evaluated in relation to treatment methods. A judgment of 'responder' was made in cases in which the thrombus subsided or disappeared within 6 h after ICT or within 72 h after IVCT or combined therapy. ICT , i.c. thrombolysis; IVCT, i.v. coronary thrombolysis. (■), non-responsive; (▨), responsive.

approximately dividing the length of time after thrombus formation into three categories: several hours; several days; and ≥1 week.

In the 'within several hours' group, six of nine patients responded regardless of the treatment method used. In the 'within several days' group, three of seven patients responded to treatment. In the '≥1 week' group, one of three patients responded to treatment. This suggests that response to thrombolytic therapy is better when the treatment is started soon after thrombus formation. When response was analyzed in relation to treatment method, the response rate to IVCT was high even when considerable time (≥1 week) had elapsed since thrombus formation. ICT alone and ICT combined with IVCT were effective only in patients treated within several hours after thrombus formation, although the small sample size of this survey does not allow the drawing of definite conclusions about the efficacy of these therapies.

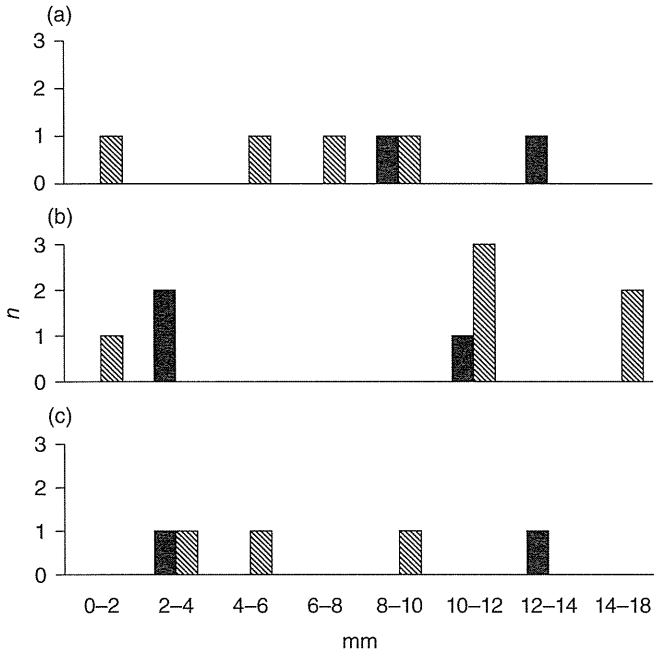

Fig. 2 Response to treatment method according to thrombus size: (a) i.c. thrombolysis ($n = 6$); (b) i.v. coronary thrombolysis ($n = 9$); (c) combined therapy ($n = 5$). In the 20 patients managed at 11 facilities, selected on the basis of secondary survey results, responses to each treatment method were evaluated in relation to thrombus size. Thrombus size was defined as the maximum dimension (diameter) in the direction perpendicular to the course of the coronary artery. (■), non-responsive; (▨), responsive.

Table 1 lists the drugs used at each facility, dose levels, and the doses recommended in relevant guidelines.[11] Although the use of t-PA for ICT is not stated in the guidelines and is not covered by health insurance, the secondary survey confirmed the use of t-PA for ICT at five facilities, including the authors' institution, among the 11 surveyed. The drugs used for ICT and their doses (guideline recommendations) were monteplase, 10 000–50 000 U/kg (recommended dose for IVCT, 27 500 U/kg); alteplase, 50 000 U/kg (recommended dose for IVCT, 290 000–435 000 U/kg); and tisokinase, 40 000 U/kg (recommended dose for IVCT, 25,000U/kg). These drugs were given repeatedly via the coronary artery (2–4 doses) in many cases. No serious hemorrhagic complications were seen following use of these drugs. In the existing guidelines, the recommended use of urokinase for ICT is up to four doses at 4000–10 000 U/kg per dose. In the present survey, urokinase was used five times at maximum at a dose of 4000–50 000 U/kg.

For IVCT, t-PA was not used at a dose exceeding the recommended level, but was used in some cases for 3 consecutive days at maximum. The use of urokinase varied more markedly among facilities, including treatment at a dose of 60 000 U at maximum (recommended dose for IVCT, 10 000–16 000 U/kg) and a maximum frequency of 5 consecutive days. No complications,

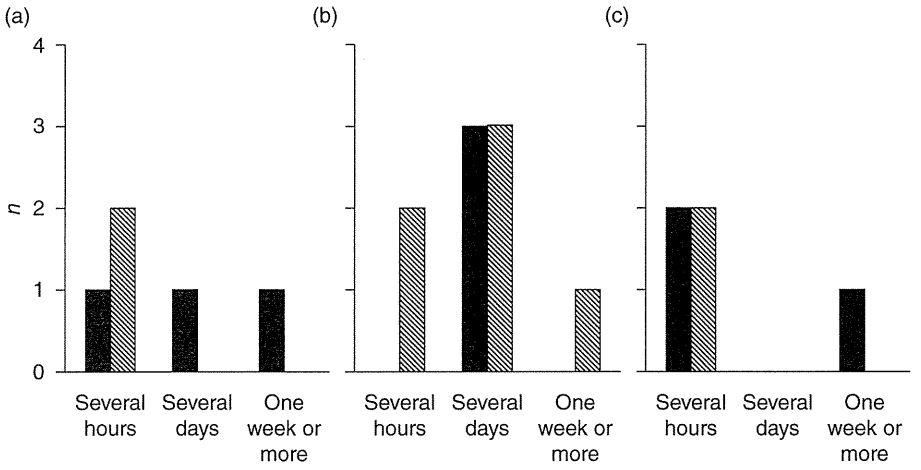

Fig. 3 Treatment response according to estimated length of time from thrombus formation until the start of treatment: (a) i.c. thrombolysis ($n = 5$); (b) i.v. coronary thrombolysis ($n = 9$); (c) combined therapy ($n = 5$). One patient with insufficient data was excluded from the 20 cases managed at 11 facilities selected on the basis of the secondary survey results. The responses of the remaining 19 patients to the treatment methods were evaluated in relation to the estimated length of time from thrombus formation until the start of treatment using an approximate rough three-category scale (several hours, several days, and ≥1 week). (■), non-responsive; (▨), responsive.

however, were noted for urokinase treatment. Thus, despite the use of t-PA for ICT (not recommended in the guidelines) or its repeated use for KD, no serious adverse reactions or complications were observed.

Discussion

Although existing guidelines mention thrombolytic therapy for patients with KD, no detailed recommendations or criteria are available for this therapy at present. Given these circumstances, we investigated the drugs used for this therapy, how they were used, and other relevant factors.

Thrombolytic drugs used for coronary aneurysm thrombosis associated with KD

Giant coronary aneurysms associated with KD are likely to cause thrombus formation despite various thrombolytic therapies, possibly leading to AMI. Drugs used to prevent this type of thrombosis or achieve thrombolysis are discussed here.

First, given that KD involves activation of platelets, anti-platelet drugs are necessary to prevent stimulation of thrombus formation via platelet activation. The most common drug used for this purpose is acetylsalicylic acid (ASA). ASA inhibits the production of thromboxane, thereby suppressing platelet aggregation. Regardless of the presence/absence of coronary aneurysm, KD patients are treated with this drug at a dose of 30–50 mg/kg per day during the acute stage and the dose is then reduced after the fever subsides. In Japan, the recommendation is to give ASA orally at a dose of 5 mg/kg per day for 2 months after disease onset, followed by a maintenance dose of 30–50 mg/kg per day for the purpose of producing anti-platelet effects.[12] In cases of aneurysm development, ongoing treatment with this drug is necessary. In cases of medium-size or giant aneurysm and thrombus

Table 1 Drugs used at each facility and dose levels

		ICT ($n = 8$)	IVCT ($n = 15$)
t-PA	A	▪ 50 000 IU/kg × 3 doses	▪ 400 000 IU/kg/day × 1 day ▪ 300 000 IU/kg/day × 3 days 290 000–435 000 IU/kg
	M	▪ 30 000–50 000 IU/kg 3 doses in total ▪ 10 000 IU/kg × 2 doses	▪ 27 500 IU/kg × 1–3 doses 27 500 IU/kg
	T	▪ 40 000 IU/kg × 3–4 doses 25 000 IU/kg	–
UK		▪ 4 000 IU/kg × 2 doses ▪ 15 000 IU/kg × 1–5 doses ▪ 50 000 IU/kg × 1–5 doses 4 000–10 000 IU/kg × up to 4 doses	▪ 4 000 IU/kg × 1–5 days ▪ 7 000 IU/kg × 1 day ▪ 16 000 IU/kg × 1–5 days ▪ 60 000 IU/kg/day × 5 days 10 000–16 000 IU/kg

Underline, guideline-recommended dose levels. A, alteplase; ICT, i.c. thrombolysis; IVCT, i.v. coronary thrombolysis; M, monteplase; T, tisokinase; t-PA, tissue-type plasminogen activator; UK, urokinase.